IV -B (2)

SANDIA REPORT SAND80-2639 • Unlimited Release • UC-70
Reprinted August 1982

Thermal Analysis of Nuclear Waste Emplacement in Welded Tuff

Brenda S. Langkopf

Prepared by
Sandia National Laboratories
Albuquerque, New Mexico 87185 and Livermore, California 94550
for the United States Department of Energy
under Contract DE-AC04-76DP00789

Issued by Sandia National Laboratories, operated for the United States Department of Energy by Sandia Corporation.

Printed in the United States of America
Available from
National Technical Information Service
U.S. Department of Commerce
5285 Port Royal Road
Springfield, VA 22161

NTIS price codes
Printed copy: A03
Microfiche copy: A01

SAND80-2639
Unlimited Release
Printed December 1981
Reprinted August 1982

Distribution
Category UC-70

Thermal Analysis of Nuclear Waste Emplacement in Welded Tuff

Brenda S. Langkopf
NNWSI Geotechnical Projects Division 4537
Sandia National Laboratories
Albuquerque, NM 87185

Abstract

Welded tuff is being evaluated as a possible medium in which to store nuclear waste. This report analyzes the heat effects of emplacing radioactive waste in welded tuff below the water table at Yucca Mountain on the Nevada Test Site (NTS). One-, two-, and three-dimensional calculations were used to evaluate the heat effects of spent fuel (SF) and commercial high-level waste (CHLW) in three regions: the very-near field, the room and pillar, and the far field. It was assumed that the canistered waste was placed in a borehole with no additional waste packaging. As a result of the calculations, interim reference-repository conditions of a gross thermal loading (GTL) of 100 kW/acre and a 20% extraction ratio (ER) were defined for both SF and CHLW. For these conditions, far-field temperatures remain below 100°C and those in the room-and-pillar domain below 120°C. In the very-near field, canister centerline temperatures are 195°C for SF and 295°C for CHLW; borehole wall temperatures are 184°C for SF and 222°C for CHLW. (The room-and-pillar and far-field temperatures are recognized as upper limits.) Once a full waste package is defined, canister loading may have to be reduced to prevent excessively high temperature within the waste package.

Contents

Figures

Figures (cont)

Tables

Glossary of Abbreviations and Acronyms

1-D	One-dimensional
2-D	Two-dimensional
3-D	Three-dimensional
CHLW	Commercial high-level waste
CL	Centerline
ER	Extraction ratio
GTL	Gross thermal loading
MIDES-WG	Mine Design Study Working Group
NTS	Nevada Test Site
NNWSI	Nevada Nuclear Waste Storage Investigation
RRC-IWG	Reference Repository Conditions—Interface Working Group
SF	Spent fuel
SNL	Sandia National Laboratories
USGS	US Geological Survey

Thermal Analysis of Nuclear Waste Emplacement in Welded Tuff

Introduction

As part of the Nevada Nuclear Waste Storage Investigations (NNWSI) project, welded tuff is being examined as a potential medium for the geologic isolation of nuclear waste. This report analyzes the thermal impact of emplacing radioactive waste, both commercial high-level waste (CHLW) and spent fuel (SF), in welded tuff. Calculations are presented for three regions: the very-near field (immediate vicinity of the canister), the room and pillar, and the far field. These calculations were completed by members of the Mine Design Study Working Group (MIDES-WG) that was organized by Division 4537 of Sandia National Laboratories (SNL), and madeup of representatives from SNL, RE/SPEC, Inc., and Texas A&M University. This preliminary report summarizes their results. New information gained through ongoing data collection and computer analyses will be evaluated to determine if it has any significant impact on results from preceding analyses. In particular, a full waste package must be introduced into the calculations as soon as details for it are available.

Background and Objectives

The thermal calculations described here were completed to help accomplish the main objectives of the MIDES-WG:

- To define the anticipated environment for a repository in welded tuff, either above or below the water table
- To identify both model and data needs for confident design of a repository in welded tuff
- To develop conceptual test plans for in-situ tests to resolve the issues identified above
- To integrate results of in-situ tests and laboratory and modeling studies into an engineering-design data package for use in a conceptual design of a repository

This report primarily addresses the first objective. However, analysis of the results has furthered all objectives by (1) establishing the thermal-property data and analysis bases; (2) establishing limits on controllable parameters [extraction ratio (ER) and gross thermal loading (GTL)] that affect the thermal field; and (3) determining scoping information on the volume of rock in which porewater is vaporized when heated.

Preliminary limits were set on the ER and GTL to reduce the number of calculations needed in subsequent thermal-mechanical analyses, and to develop a single set of thermal analyses for use in defining interim reference-repository conditions needed by the Reference Repository Conditions-Interface Working Group (RRC-IWG). Limits were imposed on the ER and GTL by applying available temperature criteria to temperatures resulting from the calculations. The most recently published thermal criteria were used. These include temperature limits of 375°C for zircaloy fuel cladding, 375°C for a stainless-steel canister, and 500°C for a glass waste form.[1] No meaningful thermal criteria could be identified for the emplacement medium, which is a nonzeolitized welded tuff.

The set of calculations used to determine interim reference-repository conditions also provides scoping information on the amount of rock in which porewater is vaporized as a result of waste emplacement. This is important because the thermal conductivity of water-saturated tuff is higher than that for dehydrated tuff. In the thermal calculations, it was generally assumed that tuff dehydrated and thermal conductivity decreased when the tuff reached the local boiling point of water—thus causing higher thermal gradients and temperatures near the heat source.

Calculation Conditions

Common repository geometries for rooms and pillars similar to those used in other studies[2,3] were assumed for very-near-field and room-and-pillar calculations. Two rows of single SF canisters and one row

of single CHLW canisters were assumed emplaced in vertical holes in the floors of the rooms. Figures 1 and 2 show the geometries and dimensions used in both plan and cross-sectional views.

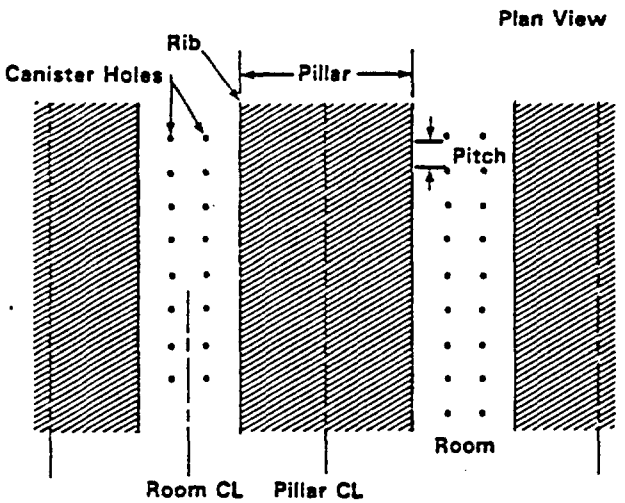

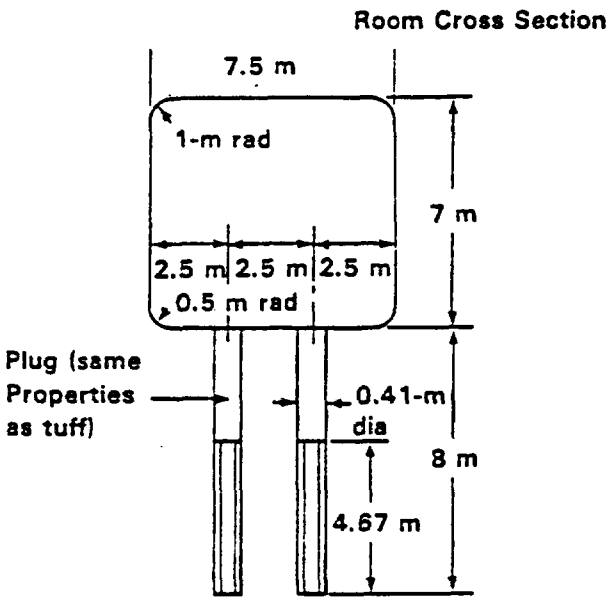

Figure 1. Initial Room Design for SF Repository in Welded Tuff

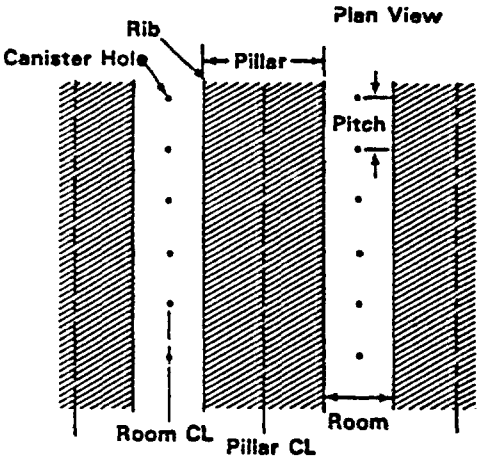

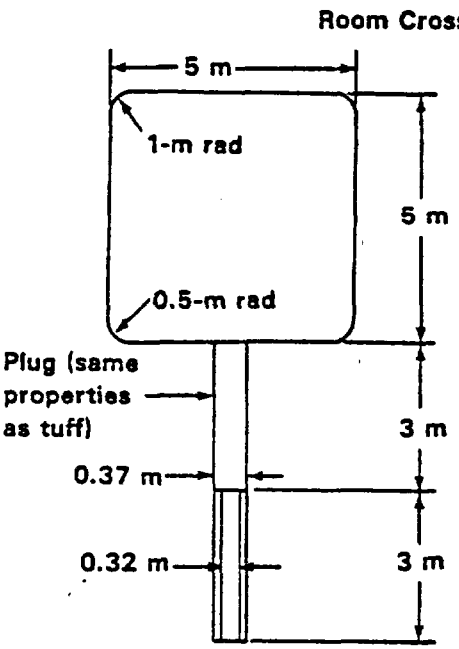

Figure 2. Initial Room Design for CHLW Repository in Welded Tuff

All the canisters were assumed simultaneously emplaced at the start of the calculations. The space above the canister in the hole was assumed backfilled by crushed tuff with the same properties as the unit in which the waste was emplaced. No waste package was

used; a 1-in. air gap surrounded the canister.* The waste itself was assumed to be 10 yr old. Initial heat generation for SF was 0.55 kW/can. For CHLW, three values of 0.50, 1.0, and 2.16 kW/can were treated. The normalized thermal output of the waste (Q/Q_o) used in the calculations is shown in Table 1 as a function of time and wasteform. Table 2 displays values for the bulk density, heat capacity, and thermal conductivity of the waste forms. Values used for the very-near-field modeling of SF were calculated by assuming the geometry and materials given in the table. Table 3 shows canister dimensions.

Table 1. Normalized Thermal Output as a Function of Waste Form and Time After Emplacement[4]

Year After Emplacement	Normalized Thermal Output CHLW	SF
0	1.0	1.0
10	0.692	0.750
15	0.600	0.681
20	0.529	0.622
30	0.402	0.525
40	0.313	0.449
50	0.246	0.387
70	0.157	0.301
100	0.0864	0.238
190	0.0296	0.137
290	0.0215	0.108
390	0.0163	0.0919
490	0.0145	0.0806
590	0.0127	0.0711
690	0.0113	0.0633
790	0.0100	0.0569
890	0.00897	0.0514
990	0.00810	0.0466
1990	0.00404	0.0247
5990	0.00230	0.0148
9990	0.00175	0.0114
50000	0.000284	0.00248
100000	0.000108	0.00081
500000	0.000085	0.00026

*The addition of a waste package will affect very-near field temperatures, but should not affect room-and-pillar or far-field temperatures. In the very-near field, the borehole-wall temperatures should be lower, and the canister centerline (CL) and skin temperatures higher if a waste package is considered. The higher temperatures for the canister CL and skin are a result of the low thermal-conductivity backfills being considered for the waste package. Although canister CL and skin temperatures increase, rock-wall temperatures will decrease because of the significantly increased area of the larger borehole. However, the major effect of the waste package will be that canister loading may be reduced to prevent excessive temperatures in the waste package.

Table 2. Material Properties of Waste Form

CHLW (vitrified)[5]

ρ_b = 3.00 Mg/m³
C_p = 0.84 J/g · °C
K = 1.21 W/m · °C

SF*[6]

ρ_b = 4.19 Mg/m³

$C_p = [690.2 + 13.38(T/100)] \times 10^{-3}$ kJ/g · °C

$$K = 0.211\left[\frac{T + 273}{100}\right]^{1.917} \text{ W/m} \cdot °C$$

Assumptions for the SF values and equations listed above are one assembly of SF/canister, containing

- 289 pins in a 17 x 7 array
- Pitch/diameter ratio between pins: 1.36
- Pin diameter: 0.97 cm
- Cladding thickness: 0.053 cm
- Pin OD: 0.81 cm
- Carbon-steel canister, air filler, zircaloy cladding, UO_2 fuel**

*These values were used in the SF calculations completed by RE/SPEC. The equivalent thermal/physical properties of the SF canister and its contents were calculated by using concentric cylinders to represent the different materials.
**The equations were calculated by using material and thermal physical properties from Reference 7 for zircaloy cladding and UO_2, and from Reference 8 for air and carbon steel.

Table 3. Canister Dimensions (Reference 5 and MIDES-WG)

CHLW Canister Description

Total Length:[5] 3.05 m
OD: 0.32 m
ID: 0.30 m
Heated length: 3.00 m
Canister material: Stainless-steel 304

SF Canister Description

Total Length:[5] 4.67 m
OD: 0.355 m
ID: 0.30 m
Heated length:[5] 3.66 m
Air-filled
Canister material: Carbon steel

Geologic Properties

The geology of the modeled repository is based on that of Yucca Mountain at the Nevada Test Site (NTS). The modeled repository was assumed to be 800 m below the ground surface, 50 m below the contact between the Bullfrog and Prow Pass Members of the Crater Flat Tuff, and 330 m below the water table. Table 4 shows the stratigraphy and thermal properties originally defined for the thermal calculations based on borehole density logs, core logs, and physical tests on core from Hole UE25a#1 at Yucca Mountain, NTS. In the calculations, the stratigraphic units encountered in UE25a#1 were assumed horizontal and representative of the stratigraphy of Yucca Mountain. UE25a#1 was drilled into but not through the Bullfrog Member; therefore, because there was no detailed geologic information about the Bullfrog, we assumed it extended to infinite depth below UE25a#1.

Core logs and borehole density logs from the US Geological Survey (USGS)[9] were complemented by laboratory bulk-property tests to subdivide the geologic units on the basis of porosity and mineralogy. Porosity values below 430 m were assigned based on a borehole density log and on core tests. Above 430 m, no density log was available and only core tests yielded measurable, usable data above this point. Few core tests were available in the Topopah Springs Member, which is located above the water table, because abundant lithophysae interfered with core recovery. Therefore, the porosity values denoted by asterisks in Table 5 had to be estimated by using the porosity of surrounding lithophysae-free zones and adding ~30% additional porosity to account for the lithophysae.

Table 4 shows that thermal conductivity and ρC_p values change when the tuff is assumed to have dehydrated by boiling of porewater. Drying of the tuff was assumed to occur over a narrow temperature range bounding the assumed local boiling point of water. Vaporization of porewater at the lower bound initiates a reduction of thermal conductivity. When temperatures within the tuff reach the lower bound of the assumed boiling temperature, energy is assumed taken out of the system by using an "effective" heat capacity derived from the heat-of-vaporization values in Table 5 and the rock volumetric heat-capacity values in Table 4. Several different methods were used to model the transition in values of thermal conductivity and heat capacity as shown in Appendix A.

Values used for the thermal conductivities of the various units were derived from unconfined thermal-conductivity tests. It was assumed that unconfined thermal conductivities are the same as the thermal conductivities at depth. Mechanical tests indicate that pore collapse should not occur at the pressures that would exist at typical repository depths; thus thermal conductivity should not change with increasing fluid-confining pressure. Thermal conductivities below temperatures of dehydration may rise, but not significantly.[11] Increased fluid pressures would, however, raise the boiling point.

Volumetric heat capacities shown in Table 4 were calculated by assuming that $\rho_b C_p = C_{pg}(1 - \phi)\,\rho_g + (C_{pw})\,(\rho_w)\,(\phi)$

where

$\rho_b C_p$ = volumetric heat capacity of the tuff
ϕ = porosity of the tuff
C_{pw} = heat capacity of water
C_{pg} = heat capacity of the grains (assumed to be 0.84 J/g · °C)
ρ_g = grain density
ρ_w = water density

The thermal diffusivity was calculated by using

$$\alpha = \frac{K}{\rho_b C_p}$$

where

α = thermal diffusivity
K = thermal conductivity of the rock
ρ_b = bulk density of the rock
C_p = specific heat of the rock

Of the values indicated in Tables 4 and 5, only those for the Bullfrog Member of the Crater Flat Tuff were used in the very-near-field and near-field calculations. The model stratigraphy used in the far-field calculations is shown in Table 6. In this table, the original stratigraphy of Table 4 was reduced by combining units of similar properties to increase computational efficiency.

Table 4. Original Stratigraphy and Material Thermal Properties for Far-Field Modeling[10]

Depth m (ft)		Porosity (%)	Bulk Density (Mg/m³)	Grain Density (Mg/m³)	$\rho_b C_p$(kJ/m³ · °C)†		K (W/m · °C)†		T_{boil} (°C) (hydrostatic)		
					$<T_{boil} - 10°$	$>T_{boil} + 10°$	$<T_{boil} - 10°$	$>T_{boil} + 10°$			
0- 53	(0- 173)	11	2.38	2.56 (m)	2.76E3	1.93E3	2.6	2.3	100	Tiva Canyon Member	Paintbrush Tuff
53- 63	(173- 208)	28	2.07	2.53 (m)	3.43E3	1.51E3	1.9	—	100		
63- 84	(208- 276)	50	1.53	2.46 (m)	3.52E3	1.05E3	0.9	0.7	100		
84-139	(276- 457)	12	2.37	2.56 (a)	2.80E3	1.88E3	2.6	2.3	100	Topopah Springs Member	
139-192	(457- 631)	50 (e)	1.78	2.56 (a)	2.09E3	1.09E3	0.85	0.7	100		
192-286	(631- 939)	12	2.37	2.57 (m)	2.80E3	1.88E3	2.6	2.3	100		
286-328	(939-1076)	50 (e)	1.78	2.56 (a)	2.09E3	1.09E3	0.85	0.7	100		
328-388	(1076-1273)	11	2.38	2.56 (m)	2.80E3	1.93E3	2.6	2.3	100		
388-401	(1273-1317)	13	2.26	2.43 (m)	2.85E3	1.80E3	1.2	1.0	100		
401-416	(1317-1364)	28	2.05	2.45 (a)	3.60E3	1.47E3	1.10	0.7	100		
416-545	(1364-1789)	31	1.97	2.40 (m)	3.73E3	1.38E3	1.05 (c) 1.10 (m)	0.67 (c) 0.71 (m)	100	Tuffaceous Beds of Calico Hills	Static Water Level = 470 m
545-560	(1789-1836)	25	2.12	2.50 (a)	3.56E3	1.55E3	1.1	0.8	175		
560-578	(1836-1897)	29	2.15	2.61 (a)	3.85E3	1.55E3	1.55	1.0	187	Prow Pass Member	Crater Flat Tuff
578-594	(1897-1950)	25	2.21	2.61 (m)	3.68E3	1.63E3	1.65	1.1	189		
594-614	(1950-2014)	18	2.34	2.62 (m)	3.35E3	1.80E3	1.80 (m) 1.80 (c)	1.39 (c) 1.33 (m)	195		
614-643	(2014-2110)	32	2.13	2.55 (m)	4.10E3	1.51E3	1.90	1.2	203		
643-697	(2110-2288)	29	2.10	2.55 (a)	3.77E3	1.51E3	2.0	1.3	214		
697-711	(2288-2333)	29	2.17	2.65 (a)	3.89E3	1.59E3	2.1	1.4	221		
711- —	(2333-∞)	23	2.28	2.66 (m)	3.64E3	1.72E3	2.4 (m) 2.35 (c)	1.65[A] (m) 1.7 (c)	223	Bullfrog Member	Repository Level = 800 m

(a) = assumed
(m) = measured
(c) = calculated
(e) = estimated value

[A] The thermal conductivity of the Bullfrog Member was changed in later calculations to 1.55 W/m°C as a result of additional laboratory data.
†In those calculations in which a condition of "no boiling" was assumed the property values were held constant by using only the values under the $<T_{boil} - 10°$ column.

Table 5. Heat Required per Unit Volume to Vaporize Porewater Present in the Tuff for the Original Stratigraphy of Yucca Mountain*

Depth m (ft)	Heat of Vaporization (kJ/m³) Assuming Boiling at 100°C	Heat of Vaporization (kJ/m³) Assuming Boiling at 220°C**
0- 53 (0- 173)	213E3	146E3
53- 63 (173- 208)	548E3	372E3
63- 84 (208- 276)	975E3	670E3
84-139 (276- 457)	234E3	159E3
139-192 (457- 631)	180E3	121E3
192-286 (631- 939)	234E3	159E3
286-328 (939-1076)	180E3	121E3
328-388 (1076-1273)	213E3	146E3
388-401 (1273-1317)	285E3	193E3
401-416 (1317-1364)	607E3	414E3
416-545 (1364-1789)	674E3	460E3
545-560 (1789-1836)	544E3	372E3
560-578 (1836-1897)	628E3	431E3
578-594 (1897-1950)	544E3	372E3
594-614 (1950-2014)	389E3	268E3
614-643 (2014-2110)	695E3	473E3
643-697 (2110-2288)	628E3	431E3
697-711 (2288-2333)	628E3	431E3
711- ∞ (2333-∞)	502E3	343E3

*The heat-of-vaporization values shown in this table were spread over various temperature ranges and combined with the volumetric heat capacity of the rock as shown in Appendix A.

**The assumption of boiling at 220°C should be conservative above the repository depth.

Table 6. Assumed Stratigraphy and Material Thermal Properties for Far-Field Modeling[12,13]

Stratigraphy		Density	Thermal Conductivity** (W/m · °C)			Volumetric Heat Capacity* ($\rho_b C_\rho$ x 10^4 kJ/m^3 · °C)		
Material*	Depth (m)	(Mg/m^3)	$T<T_{boil}-10°$	$T_{boil}-10°<T<T_{boil}+10°$	$T>T_{boil}+10°$	$T<T_{boil}-10°$	$T_{boil}-10°<T<T_{boil}+10°$	$T>T_{boil}+10°$
1	0- 53	2.380	2.60	2.45	2.30	0.276	1.320	0.188
2	53- 84	1.704	0.85	0.78	0.70	0.198	1.053	0.109
1	84-139	2.380	2.60	2.45	2.30	0.276	1.320	0.188
2	139-192	1.704	0.85	0.78	0.70	0.198	1.053	0.109
1	192-286	2.380	2.60	2.45	2.30	0.276	1.320	0.188
2	286-328	1.704	0.85	0.78	0.70	0.198	1.053	0.109
1	328-401	2.380	2.60	2.45	2.30	0.276	1.320	0.188
3	401-560	1.990	1.10	0.91	0.71	0.296	3.497	0.146
4	560-614	2.340	1.67	1.41	1.15	0.354	3.156	0.167
5	614-711	2.120	2.00	1.64	1.28	0.347	3.487	0.151
6	711-∞	2.280	2.40	2.03	1.65	0.364	2.778	0.172

*Material units with the same numbers have similar properties.
**In those calculations in which a condition of "no boiling" was assumed the property values were held constant by using only the values under the $<T_{boil}-10°$ column.

One geothermal heat flux, 1.6 $\mu cal/cm^2 \cdot s$, was used in the appropriate calculations, but two different initial in-situ temperatures were assumed. One of the temperatures, 55°C, was calculated from assumed values of thermal conductivities for stratigraphic units in UE25a#1, combined with the assumed geothermal heat flux. The second temperature, 35°C, was based on an actual field measurement and is probably more representative of the true in-situ conditions at Yucca Mountain.[14] Therefore, the calculations done by assuming an initial temperature of 55°C are used only for comparative purposes, and the calculations done by assuming an initial temperature of 35°C are used to obtain more realistic results. In the far-field calculations, an assumed ground-surface temperature of 20°C was used.

Parameters for the Analysis

Appendix B includes three tables summarizing the thermal calculations and their input parameters. The parameters that were varied include

- GTL, from 25 to 150 kW/acre
- Waste form (both SF and CHLW)
- Boiling temperature, at either hydrostatic or atmospheric pressure
- Thermal conductivity (variations of ±20% from the nominal values were used)
- Backfill at 100 yr (saturated and unsaturated), or no backfill
- ER, 10% to 30%

These parameters and their ranges were established by the MIDES-WG. Other parameters that were considered and will be treated in future calculations include waste-package configuration, ventilation, and blast cooling. These parameters could significantly affect the thermal fields.

Description of the Models

Calculations were completed with finite-element thermal-conduction codes. Thermal convection was not modeled. Thermal radiation was modeled in the air gap between the canister and borehole wall, and in the open room, by using an effective thermal conductivity formalism to represent thermal radiation. One- and two-dimensional (1- and 2-D) models were used for the far-field calculations, and two- and three-dimensional (2-D and 3-D) models for near-field and very-near-field calculations. Figures 3a through 3e illustrate the models described below.

Each model treated the heat-producing zone differently. In the 1-D far-field model, the repository is assumed to be of infinite horizontal extent with an isothermal boundary at the ground surface and a flux boundary at the bottom of the model (Figure 3a). Heat production of the repository was generalized within a 10-m-thick heat-producing block centered at the repository depth of 800 m. The 2-D far-field model was axisymmetric, with repository heat production generalized within a 10-m-thick, 2000-acre, heat-producing disk centered 5 m below the repository depth of 800 m. This model had an isothermal boundary at its top surface, a flux boundary at the bottom, and adiabatic conditions along its vertical boundaries. One of the vertical boundaries went through the centerline (CL) of the repository; the other was far removed (Figure 3b).

In some calculations, a 2-D model was used for the room-and-pillar domain. It was planar in the X-Z dimension, with the plane perpendicular to the room and through the canister and pillar. The heat produced by the nuclear waste at a given GTL was generalized to a planar heat source with the dimensions of a canister's diameter, and height. Heat output per unit volume was determined by assigning the heat output of a single canister to a parallelepiped whose volume was determined by a canister's height, diameter, and pitch. Vertical and horizontal boundaries were adiabatic, because geothermal flux and gradient were not considered in these calculations. Horizontal boundaries were far enough from the heat source to preclude any significant increase in temperature (Figure 3c).

Another 2-D model was used for the very-near-field CHLW calculations. It was axisymmetric with an "effective radius;" i.e., the radius resulting in a circular area equivalent to the actual area heated per canister. The actual area heated by a canister is the pitch distance multiplied by the pillar CL-to-CL distance. This model had vertical adiabatic boundaries—one went through the CL of the canister; the other was far removed to preclude any temperature increase. The horizontal boundaries were far enough from the heat source to preclude temperature increase at the boundaries (Figure 3d).

In the 3-D calculations, the canisters were modeled as discrete sources. The area modeled extended from the CL of the room to the CL of the pillar. All vertical boundaries were adiabatic. Horizontal boundaries were far enough away from the heat source to preclude an increase in temperature (Figure 3e).

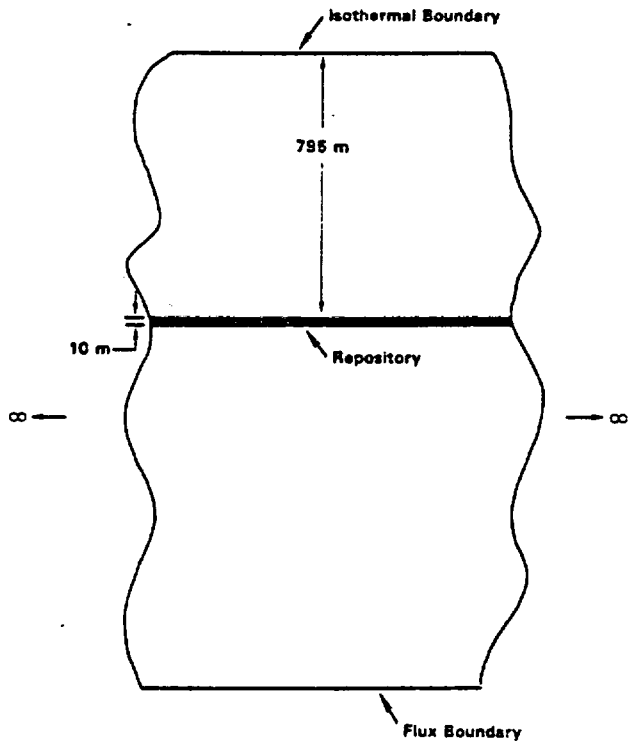

Figure 3a. 1-D Far-Field Model

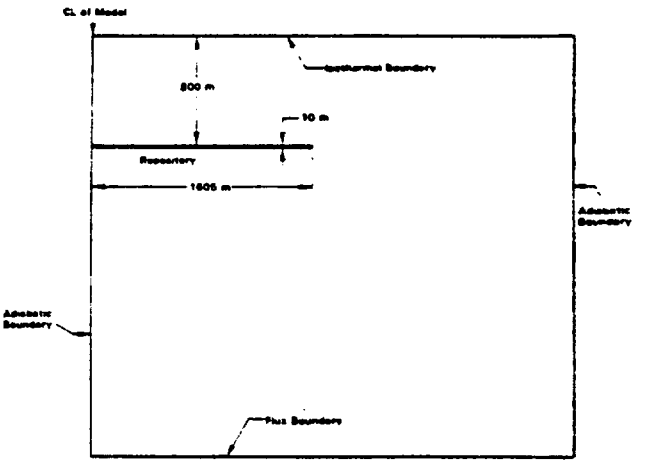

Figure 3c. 2-D Room-and-Pillar Model

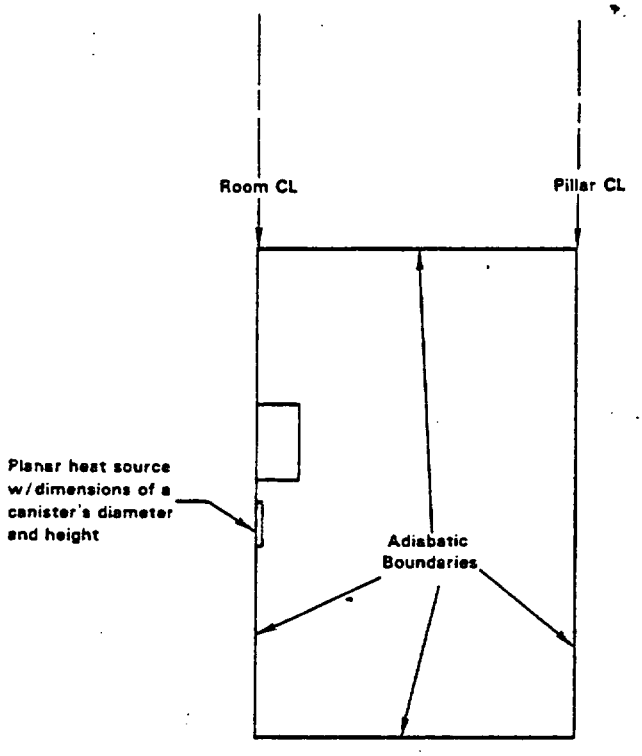

Figure 3b. 2-D Far-Field Model

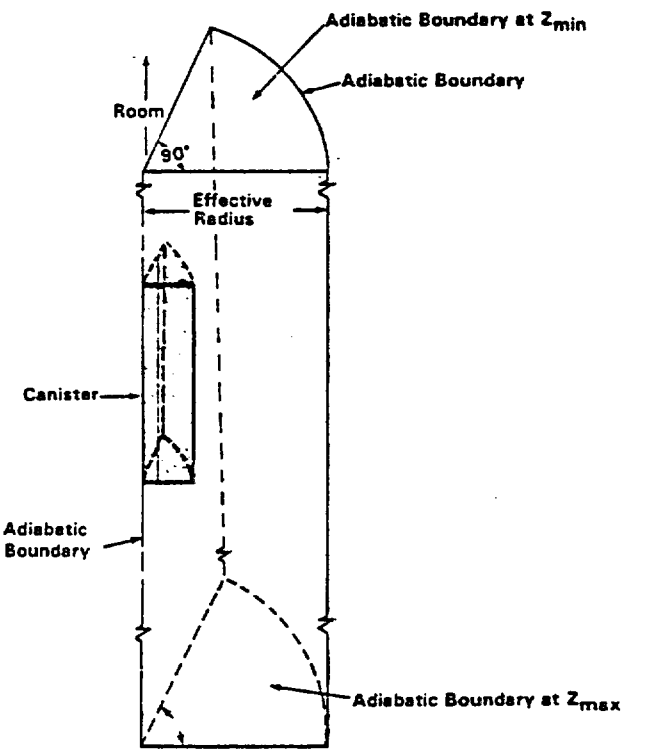

Figure 3d. 2-D Very-Near-Field Axisymmetric Model, With Effective Radius for CHLW

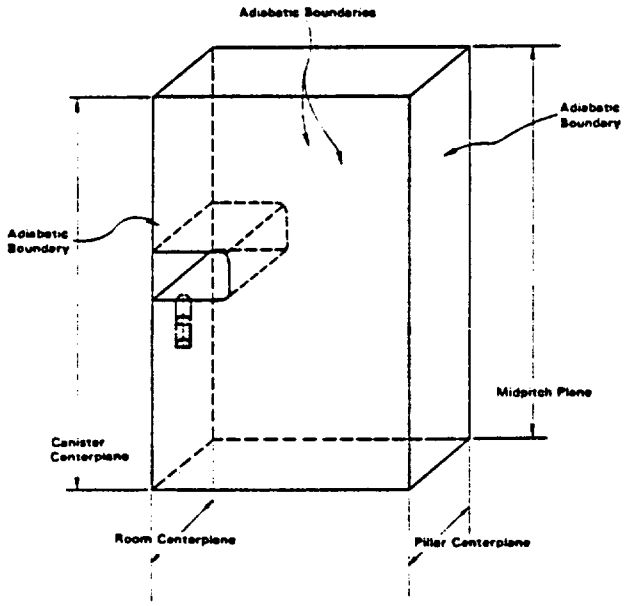

Figure 3a. 3-D Very-Near-Field and Room-and-Pillar Model for SF*

*For CHLW, the canister is centered on the centerplane of the room.

Results of the Calculations

Far-Field

Far-Field calculations were done to determine the response of the stratigraphy to waste emplacement at distances far removed from the repository for long time periods (50 to 50 000 yr). The results presented here are 2-D with hydrostatic boiling. GTL was the major parameter varied. Boiling at 225°C under repository level (800 m) hydrostatic pressure is the only boiling condition considered realistic in the far field although calculations with both boiling at atmospheric (100°C) and hydrostatic were completed. Hydrostatic rather than atmospheric boiling conditions should prevail, because the far-field water table should not be drawn down significantly. This is true as long as the permeability and recharge are large enough so that there will be no significant drawdown of the water table above the repository during the long time periods and distances of interest in the far field.

In these calculations, the hydrostatic boiling temperature was never exceeded, and the thermal conductivities of the various units remained constant. Two types of figures show the basic results of these calculations. One type (Figures 4 and 5) shows the calculated temperature rise along the vertical CL of the repository at selected times for a GTL of 100 kW/acre for SF and CHLW. At ±250 m from the repository, the largest temperature rise is 55°C for SF and 20°C for CHLW. The initial temperatures are ~25°C at +250 m and ~40°C at -250 m. Thus, temperatures should remain below 100°C within the volume defined by the planes at ±250 m. With increasing distance from the respository, temperature rises become smaller. From the figures, it is seen that a much larger volume of rock is heated by SF than by CHLW. At 50 000 yr the heated volume in Figure 5 for CHLW is 35% of the heated area for SF in Figure 4. This is a function of the heat-decay properties of SF and CHLW. SF heats a larger volume of rock over a longer time because of its slower decay rate in thermal output.

Figure 6 shows a radial temperature profile for SF waste emplacement with a GTL of 150 kW/acre at a depth of 795 m, close to the depth of the respository. Even for very high GTL, the temperatures drop significantly at the edge of the repository, and significant temperature increase is confined to within a few tens of metres of the edge.

These analyses indicate that rock temperatures should remain below 100°C except within a region extending ~250 m above and below a repository.

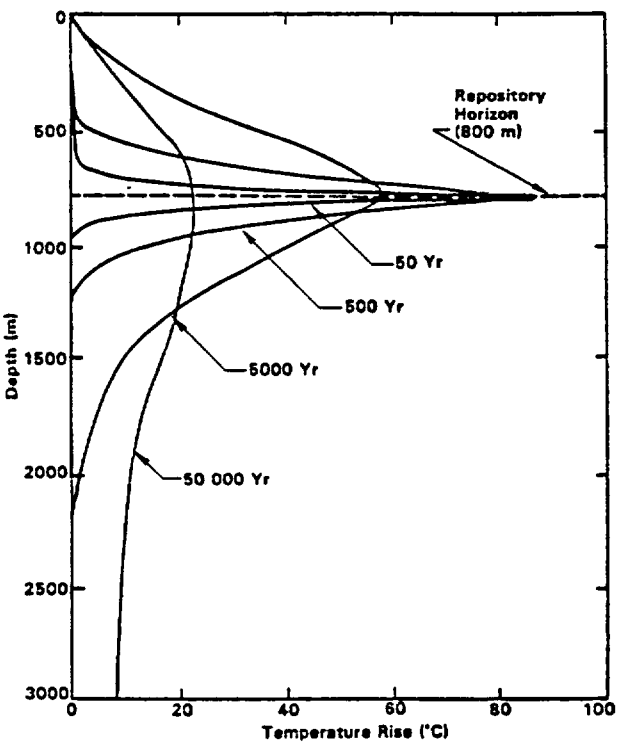

Figure 4. Temperature-Rise Profiles Along the Vertical CL of the Repository for SF (GTL = 100 kW/acre, hydrostatic boiling)[13]

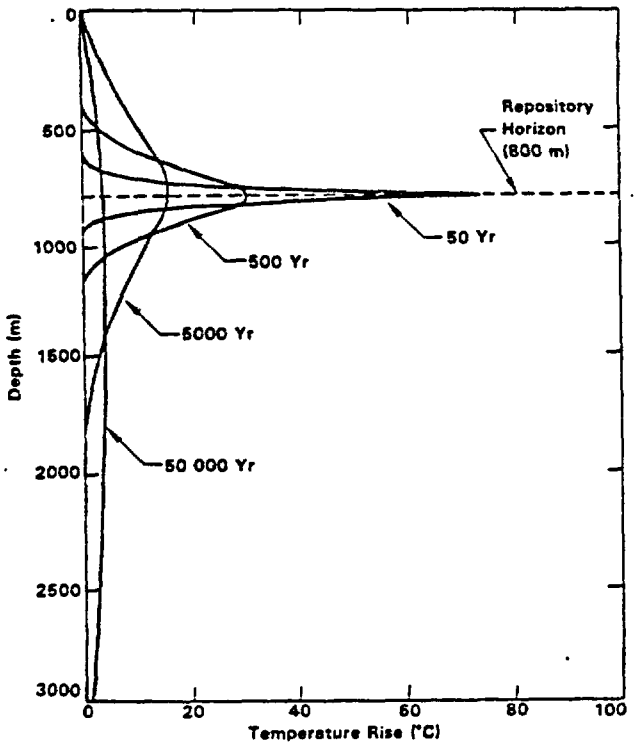

Figure 5. Temperature-Rise Profiles Along the Vertical CL of the Repository for CHLW (GTL = 100 kW/acre, hydrostatic boiling)[12]

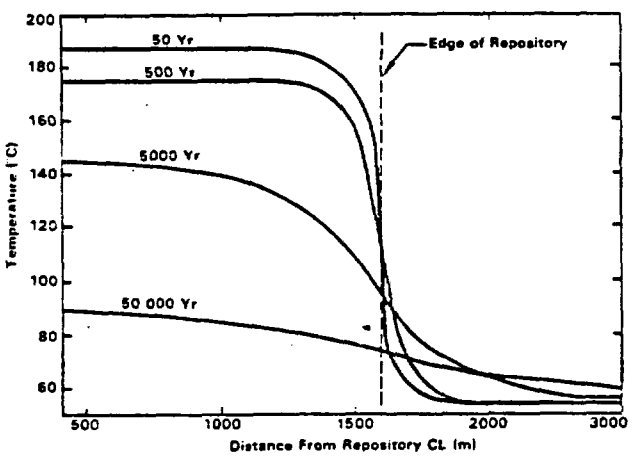

Figure 6. Radial Temperature Profile at a Depth of 795 m for SF (GTL = 150 kW/acre, 55°C initial temperature, hydrostatic boiling)[13]

Room and Pillar and Very-Near Field

Room-and-pillar calculations were completed to determine the response of rock near the storage rooms to emplacement of SF and CHLW. Times of 250 yr and less have been studied. The GTL, ER, boiling temperature, and backfill were the main parameters varied.

The temperatures in the immediate vicinity of the waste canisters and the interior of the waste package are most important in very-near-field calculations. Times of 100 yr and less have been studied; temperature peaks occur within 100 yr for both SF and CHLW. The GTL, ER, boiling temperature, and the thermal conductivity were the main parameters varied in these calculations.

Separate 2-D calculations were done for room-and-pillar and very-near-field geometries. Both geometries were considered in a single set of 3-D calculations. The 3-D calculations result in a more realistic representation of the temperature fields for both geometries.

2-D Very-Near Field — The effect of varying the thermal conductivity of tuff and canister loading of CHLW on very-near-field temperatures is shown in Figures 7a and 7b. The 2-D axisymmetric effective-radius model was used to obtain the results. The initial in-situ temperature was 55°C, the ER 20%, the GTL 75 kW/acre, and the boiling temperature 100°C. Nominal tuff conductivities of 2.4 W/m · °C below 100°C and 1.65 W/m · °C above 100°C were used, based on thermal conductivity measurements. The rest of the thermal conductivity values used were permutations of ±20% of the nominal values. Table 7 shows the values used. Several different canister loadings (0.5, 1.0, and 2.16 kW/can) were also used in these calculations.

Table 7. Thermal Conductivity Combinations Used in Very-Near-Field Calculations With Effective-Radius Model[15]

(W/m · °C) K (T <100°C)	(W/m · °C) K (T >100°C)
1.92	1.32
2.88	1.32
2.4	1.65 Nominal Case
1.92	1.98
2.88	1.98

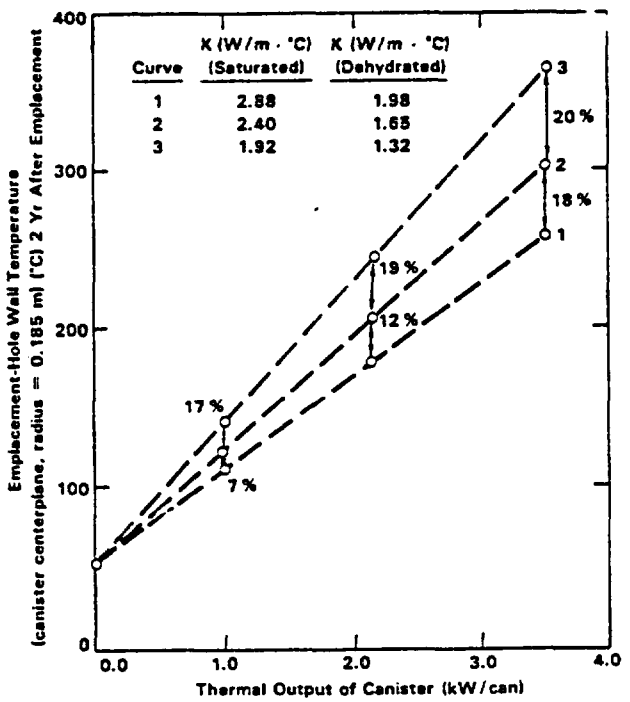

Figure 7a. Borehole Wall Temperature at 2 Yr vs Thermal Output of Canister for Nominal and Bounding Thermal Conductivity Values for CHLW (GTL = 75 kW/acre, 55°C initial temperature, 100°C boiling, 20% ER)[15]

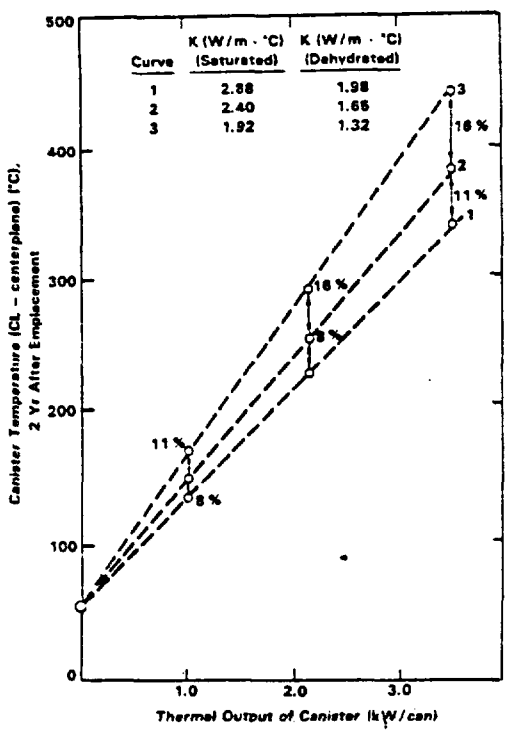

Figure 7b. Canister CL Temperature at 2 Yr vs Thermal Output of Canister for Nominal and Bounding Thermal Conductivity Values for CHLW (GTL = 75 kW/acre, 55°C initial temperature, 100°C boiling, 20% ER)[15]

Figures 7a and 7b illustrate results from the bounding and nominal calculations. Figure 7a is a plot of the borehole wall temperature at 2 yr vs the thermal output of the canister, and Figure 7b is a plot of the canister CL temperature at 2 yr vs thermal output. All the temperatures for the bounding calculations are within 20% of the nominal temperatures. Curve 3 in both figures represents the case in which the conductivities before and after boiling are reduced by 20%. It shows the greatest deviation from the nominal temperatures.

The figures also illustrate the effect of canister loading on temperatures. As canister loading decreases, the temperatures decrease linearly and there is less temperature variation in the different thermal conductivity cases considered. Figure 7b indicates that temperatures at the canister CL will reach ~370°C for a canister loading of 3.5 kW/can. This is not a favored loading, because it results in temperatures too close to the thermal criterion of 375°C for the stainless-steel canister; therefore, only the 1.0 and 2.16 kW/can canister loadings are used in followup thermal-mechanical scoping calculations.

2-D Room and Pillar (Figures 8 - 9)

The effect of backfilling the repository drift on room temperatures is illustrated in Figures 8a for SF and 9a for CHLW. Conditions for these calculations were 35°C initial in-situ temperature, an ER of 20%, and 75 kW/acre for the GTL, with a boiling temperature of 100°C. Both saturated and dry crushed-tuff backfill were used. Results for the case of saturated-tuff backfill are shown. The drift was assumed backfilled at 50 yr. Although the illustrated calculations are for saturated, crushed-tuff backfill, they are also representative of dry, crushed-tuff backfill. Two conditions make results for the two backfills nearly equivalent:

1. The backfill is emplaced at the same temperature as the drift; thus, if the drift is above the boiling temperature, both initially saturated and initially dry backfill have the same thermal conductivity.
2. Below boiling, the thermal conductivities of saturated and dry backfill, although different, are both small in comparison to the effective conductivity of the air previously in the drift.

Therefore, there is no significant difference observed as a result of emplacement of saturated vs unsaturated backfill.

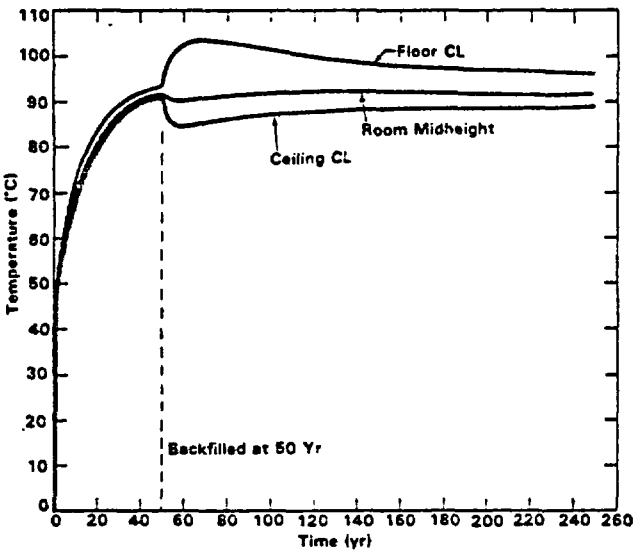

Figure 8a. Temperature Histories for Points on a Vertical Plane Perpendicular to the Room for SF (GTL = 75 kW/acre, 35°C initial temperature, 100°C boiling, saturated backfill, 20% ER)[15]

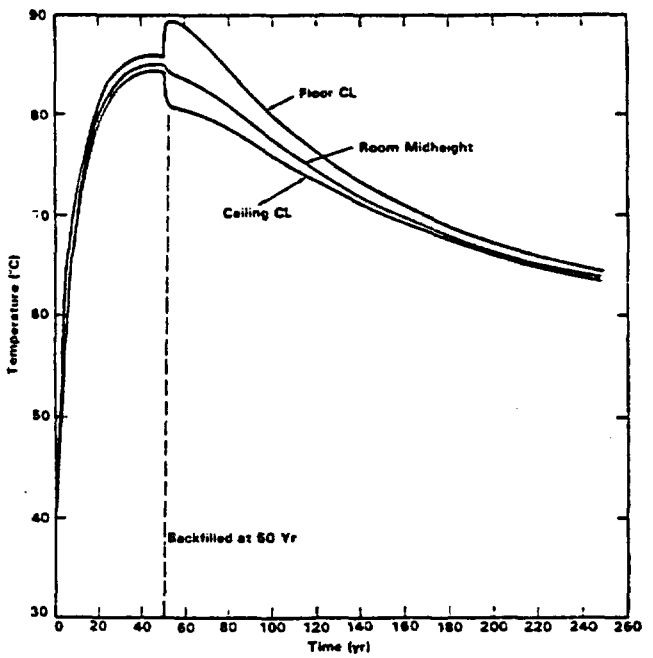

Figure 9a. Temperature Histories for Points on a Vertical Plane Perpendicular to the Room for CHLW (GTL = 75 kW/acre, 35°C initial temperature, 100°C boiling, saturated backfill, 20% ER)[15]

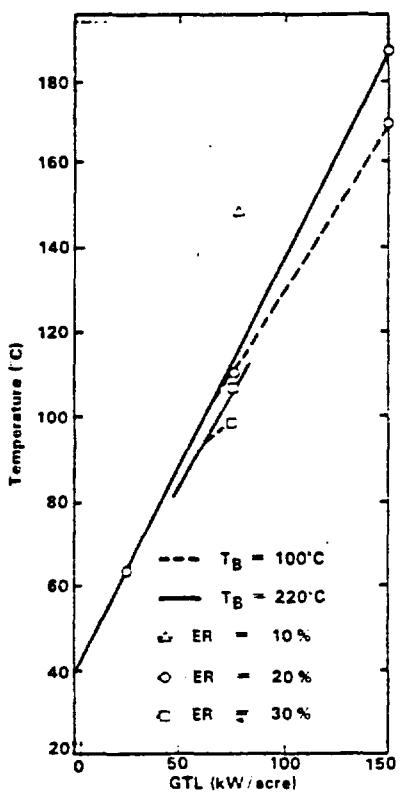

Figure 8b. Peak Floor CL Temperature for Saturated Backfill vs GTL for SF (35°C initial temperature, 20% ER)[15]

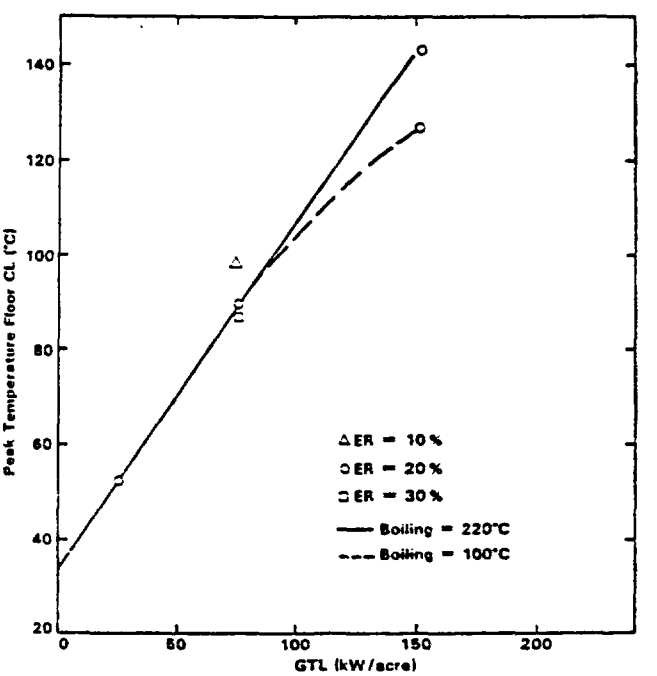

Figure 9b. Peak Floor CL Temperature for Saturated Backfill vs GTL for CHLW (35°C initial temperature, 20% ER)[15]

Backfill emplaced at a lower temperature than that of the surrounding rock acts first as a thermal sink to the ceiling and ribs; and later, when the backfill reaches the same temperature as that of the surrounding rock, it acts as a thermal barrier to conduction. In our calculations, once the backfill is emplaced at 50 yr, the floor CL temperature rises (4° to 5° for CHLW at a GTL of 75 kW/acre, and 10° for SF at a GTL of 75 kW/acre), and the ceiling CL and room midheight temperatures lower by a smaller amount. Temperatures in the pillar are not perturbed significantly by inputting the backfill. At the higher thermal loads (i.e., high GTL or low ER), the temperature changes caused by backfilling are increased and the temperature gradient through the pillar is larger. Although the temperature gradient through the pillar is inversely proportional to ER, the absolute temperature at the pillar CL varies directly with the ER.

Figures 8b for SF and 9b for CHLW show peak floor temperatures when saturated backfill is emplaced at 50 yr as a function of GTL, ER, and boiling condition. The boiling conditions assumed (hydrostatic and atmospheric) should bound the boiling conditions and temperatures that might occur in the room and pillar. The figures illustrate that, at higher GTLs, higher temperatures should be expected as the pressure in the porewater approaches hydrostatic. If the porewater is near atmospheric, the boiling temperature is lower, and temperatures at the floor CL are lower as a result of in-situ dehydration near the canisters. The figures also illustrate that peak floor temperatures are 20°C higher for CHLW and 40°C higher for SF at 10% ER than at 20% or 30% ER. The increased peak room temperatures as ER lowers are a result of the fixed room dimensions for the repository. Because room dimensions are constant, the dimension of the pillar is changed to obtain a given ER. As the pillar size is increased (i.e., the ER decreased), there is less total room area for a fixed repository area and the pitch of the canister becomes smaller to maintain a given GTL. Therefore, floor temperatures increase with a reduction in ER. An ER of 20% is assumed in thermal-mechanical scoping calculations.

3-D Very-Near Field and Room and Pillar

Selected results from 3-D calculations for SF and CHLW waste emplacement are shown in Figures 10 through 12. These results are for a GTL of 100 kW/acre, initial in-situ temperature of 35°C, 20% ER, and no backfill. A canister loading of 2.16 kW/can was used for CHLW and 0.55 kW/can for SF. Parameters of 100°C boiling and no-boil were considered. These figures include

- Temperature histories (Figures 10a through 10d) on the vertical plane through the axis of the waste canister and perpendicular to the axis of the room
- Isotherm plots (Figures 11a through 11d) on a vertical plane parallel to the axis of the room*
- Isotherm plots (Figures 12a through 12d) on the vertical plane through the axis of the waste canister and perpendicular to the axis of the room*

Time-temperature plots (Figures 10a and 10b for SF, and 10c and 10d for CHLW), indicate that CHLW emplacement causes temperatures to peak much sooner than does SF emplacement. Canister and borehole-wall temperatures peak at 2 to 3 yr for CHLW and ~20 yr for SF. In the room and pillar, peak temperatures occur at ~100 yr for SF and ~40 to 50 yr for CHLW. These plots also indicate that temperatures peak at about the same time in boiling and no-boiling calculations. Although the boiling condition does not greatly affect the time to peak temperature for the room-and-pillar or canister domain, it does change the character of the time-history curves in the canister area. The slopes of the SF curves in the near-canister area are greater both before and after the peak temperature is reached in the boiling case than in the no-boiling case. Also, slopes of the CHLW curves in the near-canister area are steeper before the peak temperature for the boiling case than for the no-boiling case.

The isotherm plots for SF (Figures 11a and 11b) indicate that within a very short time there is no longer a thermal gradient along the axis of the drift. The isotherm plots of any cross section perpendicular to the drift (Figures 12a and 12b for SF) are nearly identical, and isotherm plots (Figures 11a and 11b) along the axis of the drift are nearly straight lines. In less than a year, the thermal gradient has become very small parallel to the drift as a result of the small pitch between the canisters for SF (1.19 m), which is less than half that for CHLW (3.49 m). As a result of the differences in pitch for SF and CHLW, there is a difference in the character of isotherm plots parallel to the drift for SF and CHLW. The isotherm plots for CHLW (Figures 11c and 11d) indicate that outside the

*The isotherm plots for SF include only 80°, 90°, 100°, 110°, and 150°C, and the isotherm plots for CHLW include only 80°, 90°, 100°, and 110°C. The isotherms were too closely spaced for CHLW to show any isotherms hotter than 110°C.

canister area and at peak temperatures (~50 yr), the isotherms are almost parallel, but near the canister at 0.5, 5, and 100 yr, there is a thermal gradient. The larger pitch for CHLW causes a more noticeable thermal gradient as the temperatures rise to their peak and decline from that peak. At 0.5 and 5 yr, temperatures are increasing; at 100 yr temperatures are decreasing in the canister area.

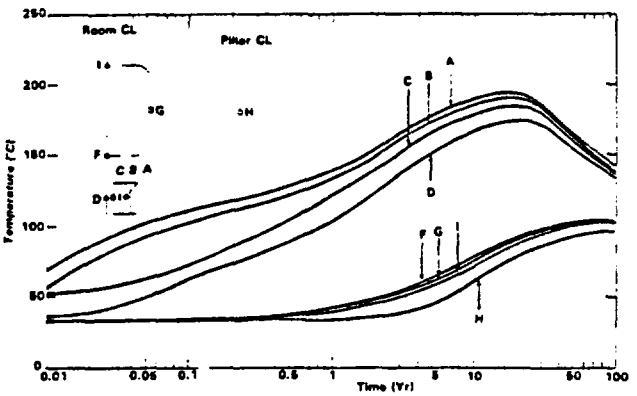

Figure 10a. Time-History Plots of Points on a Vertical Plane Through the Waste Canister Axis and Perpendicular to the Axis of the Room for SF; 100°C Boiling (GTL = 100 kW/acre, 35°C initial temperature, 20% ER)[6]

(A = canister center point; B = canister skin at canister centerplane; C = borehole wall; D = room CL at canister centerplane; F = floor at room CL; G = room wall at room midheight; H = pillar CL at room midheight; I = ceiling at room CL)

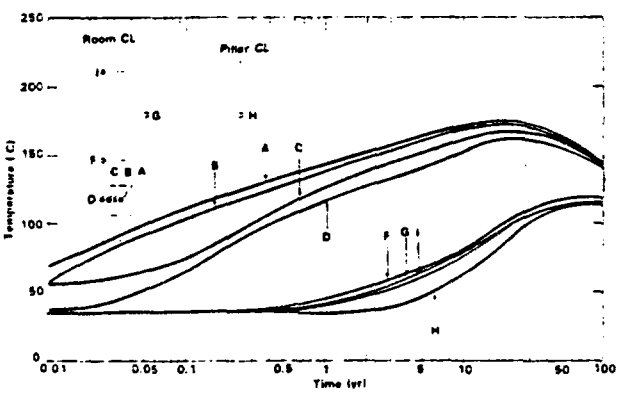

Figure 10b. Time-History Plots of Points on a Vertical Plane Through the Waste Canister Axis and Perpendicular to the Axis of the Room for SF; No Boiling (GTL = 100 kW/acre, 35°C initial temperature, 20% ER)[6]

(A = canister center point; B = canister skin at canister centerplane; C = borehole wall; D = room CL at canister centerplane; F = floor at room CL; G = room wall at room midheight; H = pillar CL at room midheight; I = ceiling at room CL)

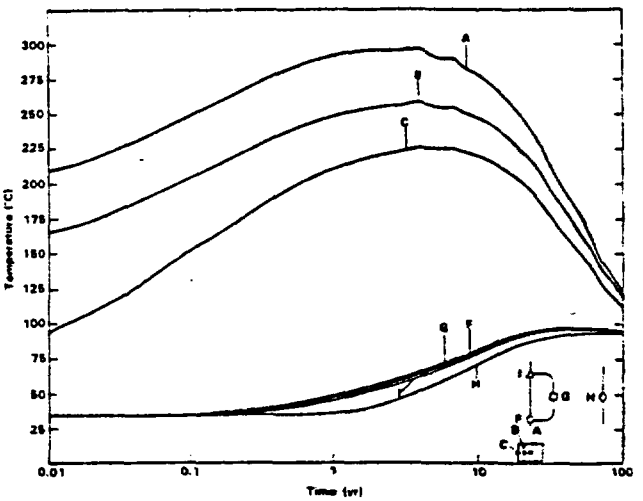

Figure 10c. Time-History Plots of Points on a Vertical Plane Through the Waste Canister Axis and Perpendicular to the Axis of the Room for CHLW; 100°C Boiling (GTL = 100 kW/acre, 35°C initial temperature, 20% ER)[16]

(A = canister center point; B = canister skin at canister centerplane; C = borehole wall at canister centerplane; F = floor at room CL; G = room wall at room midheight; H = pillar CL at room midheight; I = ceiling at room CL)

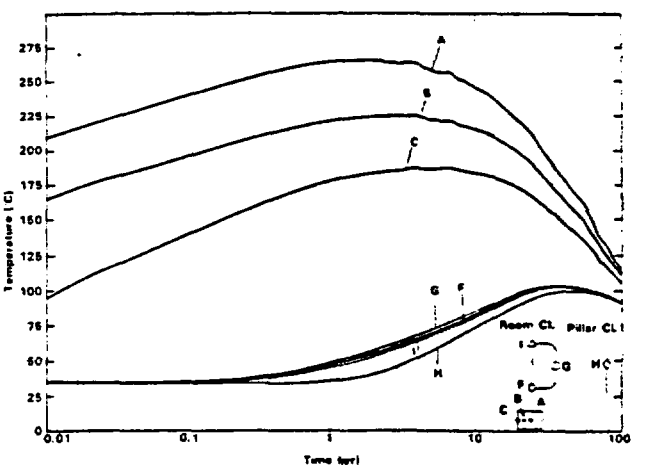

Figure 10d. Time-History Plots of Points on a Vertical Plane Through the Waste Canister Axis and Perpendicular to the Axis of the Room for CHLW; No Boiling (GTL = 100 kW/acre, 35°C initial temperature, 20% ER)[16]

Figure 11a. Isotherm Plots of the Vertical Cross Section Through the CL of the Room for SF; 100°C Boiling (GTL = 100 kW/acre, 35°C initial temperature, 20% ER)[6]

Figure 11b. Isotherm Plots of the Vertical Cross Section Through the CL of the Room for SF; No Boiling (GTL = 100 kW/acre, 35°C initial temperature, 20% ER)[6]

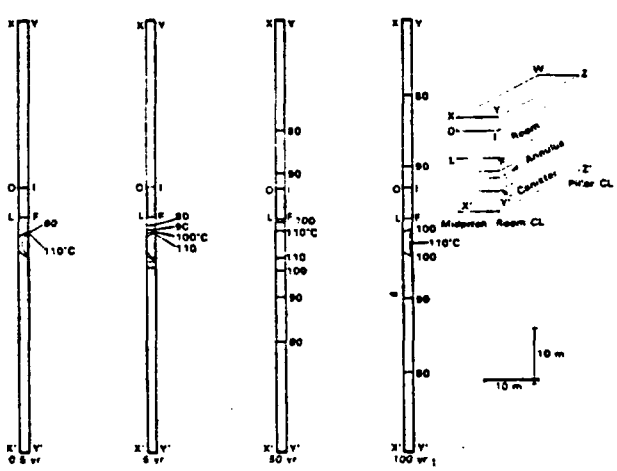

Figure 11c. Isotherm Plots of the Vertical Cross Section Through the CL of the Room and the Canister for CHLW; 100°C Boiling (GTL = 100 kW/acre, 35°C initial temperature, 20% ER)[16]

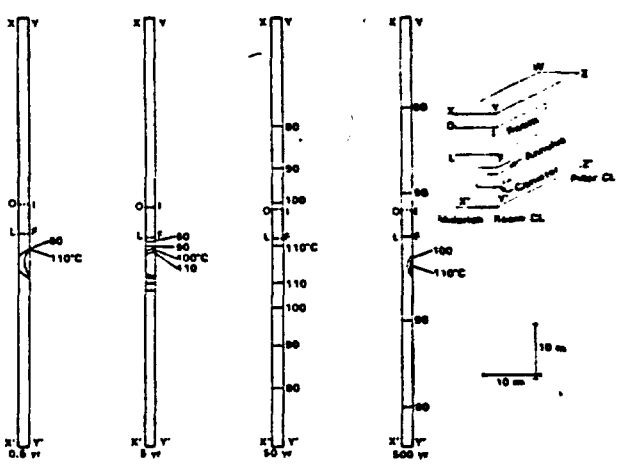

Figure 11d. Isotherm Plots of the Vertical Cross Section Through the CL of the Room and the Canister for CHLW; No Boiling (GTL = 100 kW/acre, 35°C initial temperature, 20% ER)[16]

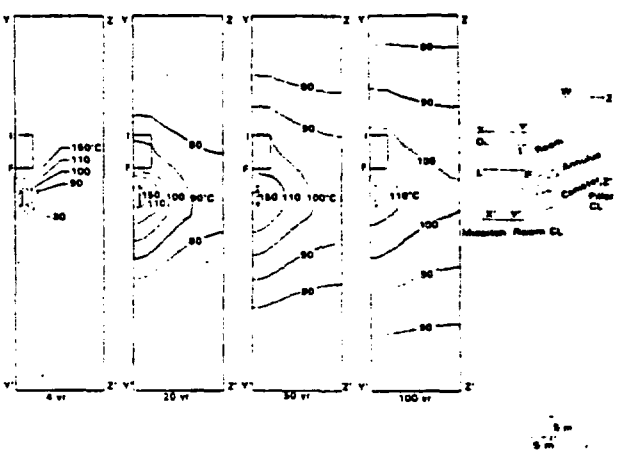

Figure 12a. Isotherm Plots of the Vertical Plane Through the Waste Canister Axis and Perpendicular to the Axis of the Room for SF; 100°C Boiling (GTL = 100 kW/acre, 35°C initial temperature, 20% ER)[6]

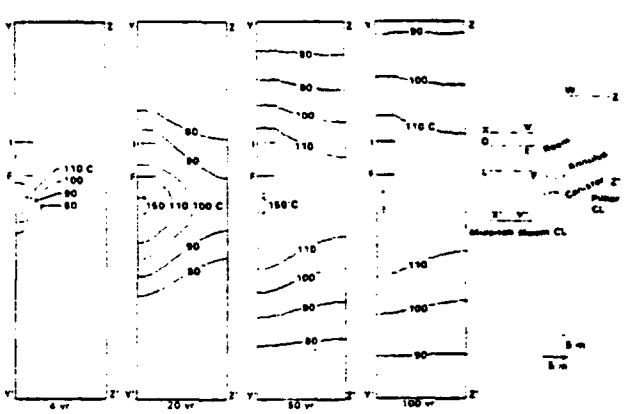

Figure 12b. Isotherm Plots of the Vertical Plane Through the Waste Canister Axis and Perpendicular to the Axis of the Room for SF; No Boiling (GTL = 100 kW/acre, 35°C initial temperature, 20% ER)[6]

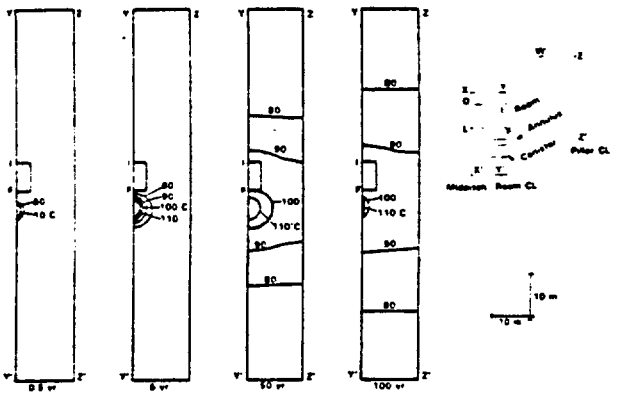

Figure 12c. Isotherm Plots of the Vertical Plane Through the Waste Canister Axis and Perpendicular to the Axis of the Room for CHLW; 100°C Boiling (GTL = 100 kW/acre, 35°C initial temperature, 20% ER)[16]

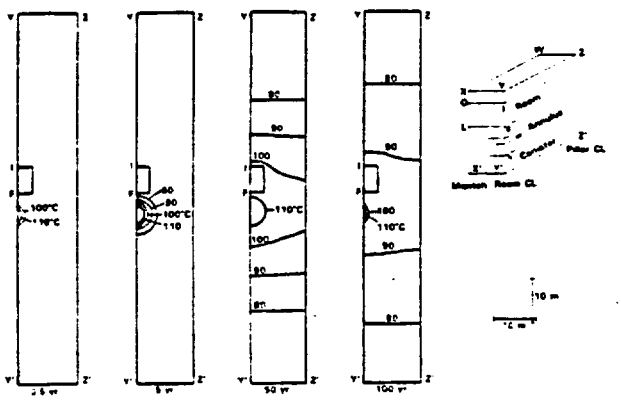

Figure 12d. Isotherm Plots of the Vertical Plane Through the Waste Canister Axis and Perpendicular to the Axis of the Room for CHLW; No Boiling (GTL = 100 kW/acre, 35°C initial temperature, 20% ER)[16]

The isotherm plots (Figures 11a and 12a for SF, and 11c and 12c for CHLW) also provide scoping information on the volume of rock in which water is vaporized during heating. Vaporization and its corresponding decrease in thermal conductivity were assumed to occur within ±10° (90° to 110°C) of the fixed atmospheric boiling temperature of 100°C in the cases in which boiling was considered. Therefore, the volume of rock dehydrated per canister can be approximated by using Figures 11a and 12a for SF and Figures 11c and 12c for CHLW. One-half the area between the 90° to 110°C isotherms and all the area within the isotherms greater than 110°C, multiplied by the pitch, gives the volume of rock dehydrated per canister of SF. The area from the CHLW curve must be doubled because there is only one row of canisters along the drift; thus only one-half the volume heated per canister is represented in the CHLW curve. The volume of rock dehydrated per canister at the approximate time of peak temperatures is ~450 m^3 for SF at 100 yr and ~520 m^3 for CHLW at 50 yr. In dehydrating these volumes of rock, ~30% of the cumulative energy output per canister of SF was used, and ~15% per canister of CHLW.

Table 8 summarizes peak temperatures as predicted by the 3-D calculations for CHLW and SF. This table first compares peak temperatures for the boiling and no-boiling cases for each waste type; then it compares percentage changes in the boiling and no-boiling case within one waste type, and similar boiling cases between waste types. How boiling affects very near-field and room-and-pillar peak temperatures is shown in this table. In the canister area, peak temperatures for CHLW and SF are 11% to 19% higher for the boiling case than the no-boiling case; in the room-and-pillar, peak temperatures for CHLW and SF are 8% to 15% lower for the boiling case. The heat removed from the tuff as a result of vaporization of the porewater at "boiling" in the very-near field causes lower temperatures in the room-and-pillar area, and the thermal conductivity that is lowered as a result of boiling causes temperatures to rise in the canister area.

Interim reference temperatures used by the RRC-IWG are based on the 3-D, 100°C boiling results analyzed above. The calculation conditions included a GTL of 100 kW/acre, 20% ER, and canister loadings of 2.16 kW/can for CHLW and 0.55 kW/can for SF. Figures 13a and 13b show plots of the canister CL temperature vs GTL for all the 3-D calculations completed with a 35°C initial in-situ temperature. These figures indicate that the canister CL temperature for both CHLW and SF, at a GTL of 100 kW/acre, is well below the only thermal criteria that are applicable. CHLW has a canister CL temperature of 295°C vs the temperature criterion of 375°C for a stainless-steel canister. Clearly, the skin temperature of the canister must be less than 295°C and is therefore well below the thermal criterion. SF has a canister CL temperature of 194°C as compared to the temperature criterion of 375°C for zircaloy cladding.*

The choice of a GTL of 100 kW/acre for a reference repository should be affected by use of a more elaborate waste package. This would increase canister temperatures and may require reduced thermal loading of the canister. The GTL might be lowered by the desire to restrict the volume of rock in which water is vaporized and the operating temperature of the room.

*It is recognized that this canister CL temperature does not relate directly to cladding temperatures. However, it is so far below the allowable maximum that explicit calculation of cladding temperature would not yield a result in excess of 375°C.

Table 8. Summary of Resulting Peak Temperatures and Percentage Changes in Peak Temperatures of CHLW and SF From 3-D Calculations (100 kW/acre, 35°C initial temperature)[6,16]

	Very-Near Field (°C)			Room and Pillar (°C)			
	Canister CL	Canister Skin	Borehole Wall	Floor	Room Midheight	Ceiling CL	Pillar CL
CHLW Boil	295	255	222	95	94	93	88
CHLW No-Boil	266	225	186	103	103	103	100
SF Boil	194	190	184	105	102	101	97
SF No-Boil	175	171	166	120	118	117	114
Temperature Change (%)							
CHLW No-Boil to Boil	+11	+13	+19	-8	-9	-10	-12
SF No-Boil to Boil	+11	+11	+11	-13	-14	-14	-15
SF Boil to CHLW Boil	+51	+34	+22	-10	-8	-8	-9
SF No-Boil to CHLW No-Boil	+51	+32	+12	-14	-13	-12	-12

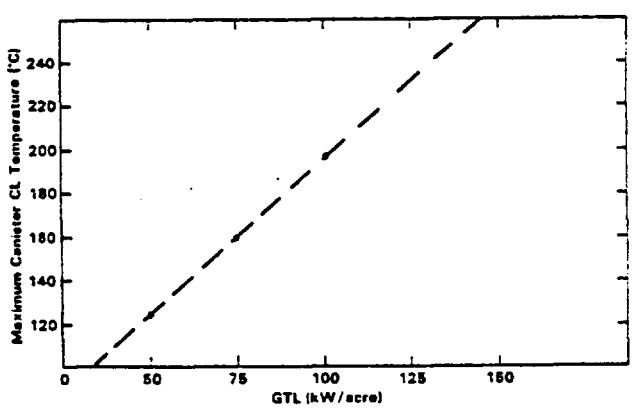

Figure 13a. Maximum Canister CL Temperature vs GTL for SF (100°C boiling, 20% ER)[6]

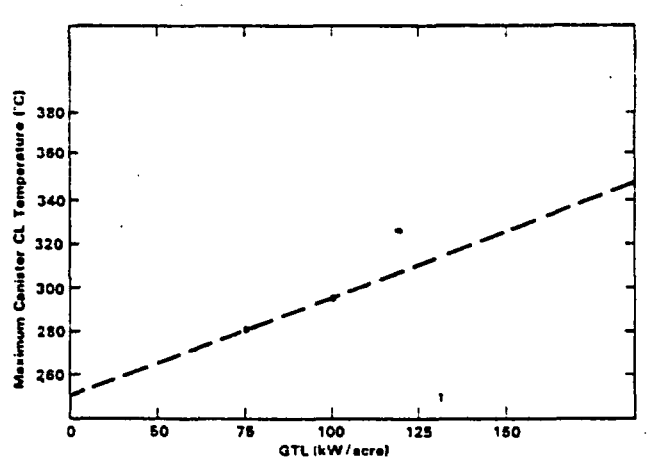

Figure 13b. Maximum Canister CL Temperature vs GTL for CHLW (100°C boiling, 20% ER)[16]

Comparison of 2-D and 3-D Calculations

In all cases where 2- and 3-D calculations were compared, the very-near-field temperatures from the 3-D calculations were ~10% higher. Comparisons have been made of the 2-D very-near-field axisymmetric-effective-radius model with a 3-D model, and of the 2-D room-and-pillar planar model with a 3-D model. In the first case (Figure 14), the 3-D model produced larger temperatures because the canisters in the 2-D model were generalized as a rectangular parallelepiped, whereas the 3-D model was able to model discrete souces of heat to more accurately represent the waste canisters. With decreasing pitch, the 2-D planar model should better represent the repository.

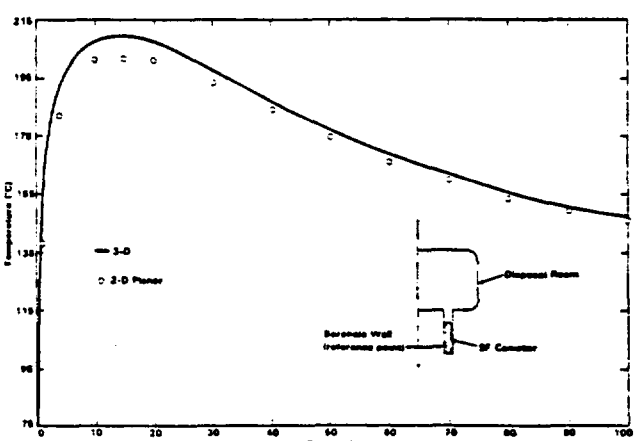

Figure 14. Comparison of 2-D and 3-D Time-History Plots of the Borehole Wall for SF (GTL = 100 kW/acre, 55°C initial temperature, 100°C boiling)[6]

The 3-D model temperatures were higher in the second case (Figure 15) because the adiabatic boundary at midpitch was closer to the canister than was the adiabatic boundary in the 2-D effective-radius model, which uses a radius that is a compromise between the midpitch and midpillar boundaries. As the pitch decreases, the effective-radius model becomes less representative of the repository.

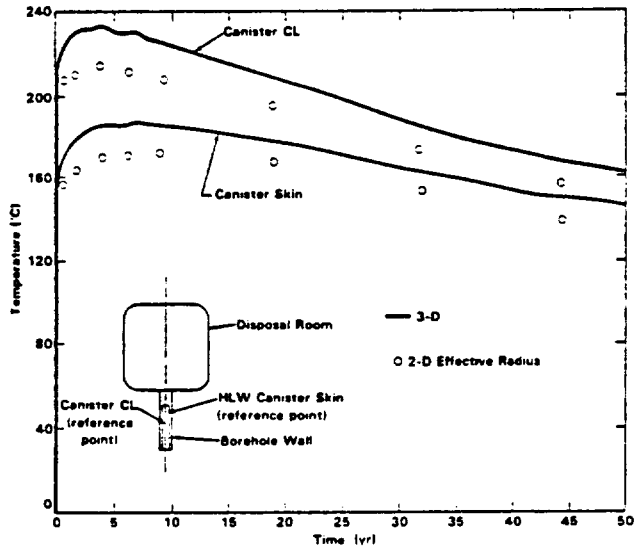

Figure 15. Comparison of 2-D and 3-D Time-History Plots of the Canister CL and Canister Skin for CHLW (GTL = 100 kW/acre, 2.16 kW/can, 35°C initial temperature, no boiling)[15]

Summary

Preliminary thermal calculations completed by the MIDES-WG include the very-near field, room and pillar, and far field. Based on thermal criteria and results from these calculations, interim reference-repository conditions were determined to define the thermal environment expected in a nonzeolitized welded-tuff repository below the water table. A reference was set of 100 kW/acre for GTL, 20% ER, 100°C boiling, 2.16 kW/can for CHLW, and 0.55 kW/can for SF.

Very-near-field 3-D calculations for these conditions indicate that the highest temperatures expected in the repository will be the peak canister CL temperatures of 295°C for CHLW and 194°C for SF, which occur at 2 to 3 yr for CHLW and at ~20 yr for SF.

Room-and-pillar 3-D calculations indicate that temperatures in the room and pillar should remain below 120°C. Peak temperatures in the room-and-pillar calculations occur at 40 to 50 yr for CHLW and ~100 yr for SF. The 3-D room-and-pillar, very-near-field calculations with 100°C boiling indicate that temperatures will be higher in the very-near-field and lower in the room-and-pillar than for no boiling.

Far-field calculations indicate that rock temperatures, except those within 250 m surrounding the repository, will remain <100°C. The far-field temperatures are well below hydrostatic boiling temperature, the only boiling temperature of importance in the far field.

References

[1]G. H. Jenks, *Maximum Acceptable Temperature of Waste and Containers During Retrievable Geologic Storage*, Y/OWI/TM-42 (Washington, DC: Office of Nuclear Waste Isolation, 1977).

[2]US Department of Energy, *Management of Commerically Generated Radioactive Waste*, DOE/EIS-0046-D, Vol 2 (Washington, DC: US DOE, April 1979).

[3]*Thermal Analyses, Vol. 19 of Technical Support for GEIS: Radioactive Waste Isolation in Geologic Formations*, Y/OWI/TM-36/19 (Washington, DC: Office of Waste Isolation, April 1978).

[4]R. A. Kisner et al, *Nuclear Waste Projections and Source Term Data for FY1977*, Y/OWI/TM-34, (Washington, DC: Office of Waste Isolation, April 1978).

[5]H. C. Claiborne, L. D. Rickertson, and R. F. Graaham, *Expected Environments in High-Level Nuclear Waste and Spent Fuel Repositories in Salt*, ORNL/TM-7201 (Oak Ridge, TN: Oak Ridge National Lab, August 1980).

[6]D. Parrish, *Very-Near-Field Thermal Analysis of a Spent Fuel Repository in Tuff*, Topical Report RSI-0144 (Rapid City, SD: RE/SPEC, Inc. unpublished); also SAND81-7211 (Albuquerque, NM: Sandia National Laboratories, in press).

[7]H. C. Claiborne and L. D. Rickertson, Draft ERE (Expected Repository Environments), (Oak Ridge, TN: Oak Ridge National Lab, 1979).

[8]A. J. Chapman, *Heat Transfer*, 2nd ed (New York: The MacMillan Co., 1967).

[9]R. W. Spengler, D. C. Muller, and R. B. Livermore, *Preliminary Report on the Geology and Geophysics of Drillhole UE25a=1, Yucca Mountain, Nevada Test Site*, Open File Report 79-1244, (Washington, DC: US Geological Survey, 1979).

[10]Written communication, A. R. Lappin of Sandia National Laboratories, December 1979.

[11]A. R. Lappin, *"Thermal Conductivity of Silicic Tuffs: Predictive Formalism and Comparison with Preliminary Experimental Results,"* SAND80-0769 (Albuquerque, NM: Sandia National Laboratories, April 1981).

[12]M. L. Klasi, J. E. Russell, W. C. McClain, and T. Brandschaug, *Far-Field Thermal Analysis of a High-Level Waste Repository in Tuff*, Topical Report RSI-0137 (Rapid City, SD: RE/SPEC, Inc., unpublished); also SAND81-7209 (Albuquerque, NM: Sandia National Laboratories, in press).

[13]M. L. Klasi, W. C. McClain, and T. Brandschaug, *Far-Field Thermal Analysis of a Spent Fuel Repository in Tuff*, Topical Report RSI-0128 (Rapid City, SD: RE/SPEC, Inc., unpublished); also SAND81-7210 (Albuquerque, NM: Sandia National Laboratories, in press).

[14]J. H. Sass, Arthur H. Lachenbruch, and C. W. Mase, *Analysis of Thermal Data From Drill Holes UE25a#3 and UE25a#1, Calico Hills and Yucca Mountain, Nevada Test Site*, Open File Report 80-826, (Washington, DC: USGS, 1980).

[15]D. K. Gartling, R. R. Eaton, and R. K. Thomas, *Preliminary Thermal Analyses for a Nuclear Waste Repository in Tuff*, SAND80-2813 (Albuquerque, NM: Sandia National Laboratories, April 1981).

[16]W. Sundberg and R. R. Eaton, *3-D Thermal Analysis for a Conceptual High-Level Waste Repository in Tuff*, SAND81-0215 (Albuquerque, NM: Sandia National Laboratories, in press).

APPENDIX A

Methods Used to Change Thermal Conductivity and Heat of Vaporization

This appendix illustrates different ways that the thermal conductivities and volumetric heat capacities of the tuff were changed as a function of temperature in the calculations. The figures model the properties of the tuff rock as it changes from saturated to dehydrated at boiling as a result of porewater vaporization.

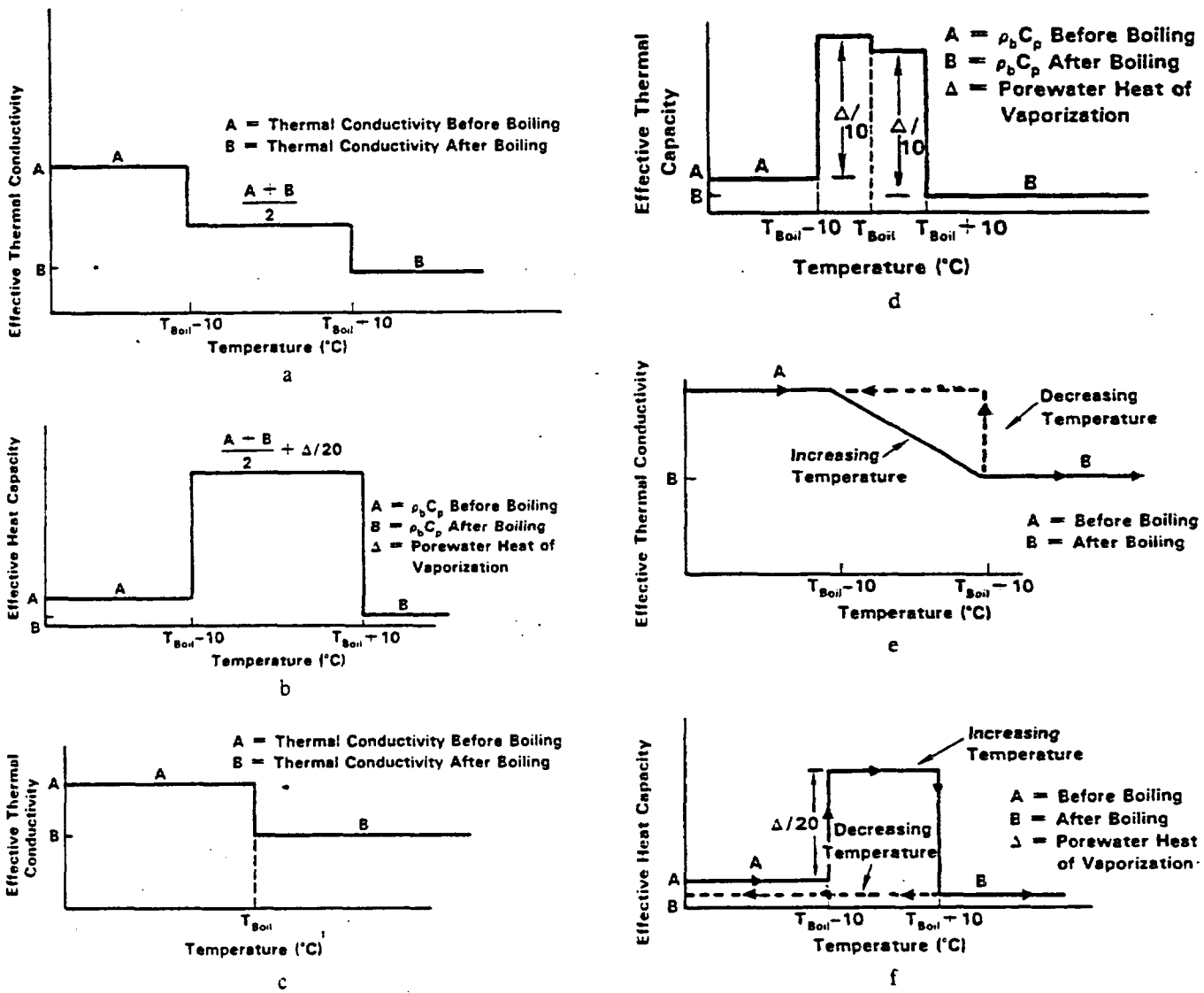

Figure A-1. Methods By Which Thermal Conductivity and Heat Capacity of Welded Tuff Were Modeled Upon Vaporization of Porewater.

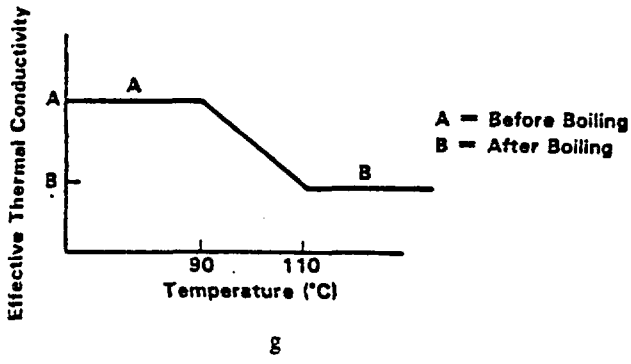

g

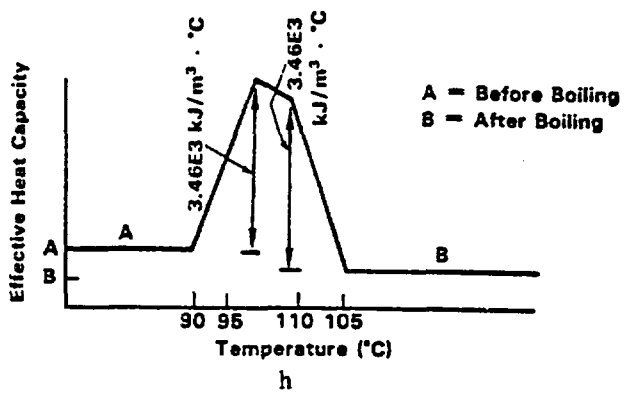

h

Figure A-1. (cont)

APPENDIX B

Summary of Thermal Calculations and Their Parameters

This appendix summarizes all the parameters used in the thermal calculations.

Table B-1. Summary of All Parameters Input in Far-Field Calculations

Type of Model	Waste Form	Thermal Loading (kW/acre)	Boiling Parameter (°C)	Time Range (yr)	Rock Thermal Conductivity (W/m · °C; $T < T_{boil} - 10°C$)	Rock Thermal Conductivity (W/m · °C; $T > T_{boil} + 10°C$)	Figure in Appendix A Showing How Rock Thermal Conductivity Was Changed	Rock $\rho_r C_p$ (kJ/m³ · °C; $T < T_{boil} - 10°C$)	Rock $\rho_r C_p$ (kJ/m³ · °C; $T > T_{boil} + 10°C$)	Figure in Appendix A Showing How $\rho_r C_p$ Was Changed	Initial Temperature at Repository Horizon (°C)	Investigator	Reference
2-D axisymmetric	SF	25,50,75, 100,150	Hydrostatic†	0 - 50 000	2.4	2.4	A-1	3.64E3	1.72E3	A-2	55	RE/SPEC	13
2-D axisymmetric	SF	50,75,100, 150	100	0 - 50 000	2.4	1.65	A-1	3.64E3	1.72E3	A-2	55	RE/SPEC	13
2-D axisymmetric	CHLW	25,50,75, 100	Hydrostatic†	0 - 50 000	2.4	1.65	A-1	3.64E3	1.72E3	A-2	55	RE/SPEC	12
2-D axisymmetric	CHLW	75,100	100	0 - 50 000	2.4	1.65	A-1	3.64E3	1.72E3	A-2	55	RE/SPEC	12
1-D axisymmetric	CHLW	25,75,100, 150	Hydrostatic†	0 - 1000	2.4	1.65	A-5	3.64E3	1.72E3	A-6	55	Texas A&M	12
1-D axisymmetric	CHLW	75,100,150	100	0 - 1000	2.4	1.65	A-5	3.64E3	1.72E3	A-6	55	Texas A&M	12

†The hydrostatic boiling temperature was never exceeded so in essence these calculations are "no boil" calculations.

Table B-2. Summary of All Parameters Input in Room-and-Pillar 2-D Planar Calculations*

Waste Form	Thermal Loading (kW/acre)	Boiling Parameter (°C)	ER (%)	Time Range (yr)	Rock Thermal Conductivity (W/m · °C; T_{bnd} 10°C)	Rock Thermal Conductivity (W/m · °C; T_{bnd} 10°C)	Figure in Appendix A Showing How Thermal Conductivity Was Changed	Rock $\rho_R C_p$ (kJ/m³ · °C; $T < T_{bnd}$ 10°C)	Rock $\rho_R C_p$ (kJ/m³ · °C; $T > T_{bnd}$ 10°C)	Figure in Appendix A Showing How $\rho_R C_p$ Was Changed	Air in Room Pseudo Thermal Conductivity Used (W/m · °C)	Waste Thermal Conductivity (W/m · °C)	Air ρC_p (kJ/m³ · °C)	Waste ρC_p (kJ/m³ · °C)	Initial In Situ Temperature at Repository Horizon (°C)	Backfill Parameter	Backfill Thermal Conductivity W/m · °C and $T < T_{bnd}$ 10°C	Ba Th Condu W/m · T < T
SF	25	100	10	0 - 250	2.4	1.65	A-3	3.64E3	1.72E3	A-4	25	1.21	1.00	2.5E3	35	Saturated	1.18	
SF	75	100	10,30	0 - 250	2.4	1.65	A-3	3.64E3	1.72E3	A-4	25	1.21	1.00	2.6E3	35	Saturated	1.18	
SF	75	100	10,30	0 - 250	2.4	1.65	A-3	3.64E3	1.72E3	A-4	25	1.21	1.00	2.5E3	35	Dry	0.48	
SF	75	220	10,30	0 - 250	2.4	1.65	A-3	3.64E3	1.72E3	A-4	25	1.21	1.00	2.5E3	35	Saturated	1.18	
SF	25,75,150	100	20	0 - 250	2.4	1.65	A-3	3.64E3	1.72E3	A-4	25	1.21	1.00	2.5E3	35	Saturated	1.18	
SF	25,75,150	100	20	0 - 250	2.4	1.65	A-3	3.64E3	1.72E3	A-4	25	1.21	1.00	2.5E3	35	Dry	0.48	
SF	25,75,150	220	20	0 - 250	2.4	1.65	A-3	3.64E3	1.72E3	A-4	25	1.21	1.00	2.5E3	35	Saturated	1.18	
CHLW	25,75,150	100	20	0 - 250	2.4	1.65	A-3	3.64E3	1.72E3	A-4	25	1.21	1.00	2.5E3	35	Saturated	1.18	
CHLW	25,75,150	220	20	0 - 250	2.4	1.65	A-3	3.64E3	1.72E3	A-4	25	1.21	1.00	2.5E3	35	Saturated	1.18	
CHLW	25,75,150	100	20	0 - 250	2.4	1.65	A-3	3.64E3	1.72E3	A-4	25	1.21	1.00	2.5E3	35	Dry	0.48	
SF	75,150	100	20	0 - 250	2.4	1.65	A-3	3.64E3	1.72E3	A-4	25	1.21	1.00	2.5E3	55	Saturated	1.18	
SF	75,150	220	20	0 - 250	2.4	1.65	A-3	3.64E3	1.72E3	A-4	25	1.21	1.00	2.5E3	55	Saturated	1.18	
CHLW	25,75,150	100	20	0 - 250	2.4	1.65	A-3	3.64E3	1.72E3	A-4	25	1.21	1.00	2.5E3	55	Saturated	1.18	
CHLW	25,75,150	220	20	0 - 250	2.4	1.65	A-3	3.64E3	1.72E3	A-4	25	1.21	1.00	2.5E3	55	Saturated	1.18	
SF	75,100	100	20	0 - 100	2.4	1.55	A-1	3.64E3	1.72E3	A-2	55,61**	(A)	(C)	(B)	35	None		

*The 3-D Calculations in Table B-3 include the room and pillar.
**Listed in order used for various GTL's.

(A) $0.211 \cdot \left(\frac{T + 273}{100}\right)^{1.97}$ = K in W/m · °C, T = °C

(B) $4.194 [690.2 + 13.38 (T/100)] \cdot \rho C_p$ in kJ/m³ · °C, T = °C

(C) $\left.\begin{array}{l} \text{if } 0 \le T/T_o < 1.0 \text{ then } \rho = 1.289 \exp(0.31\, T/T_o) \\ \text{if } 1.0 \le T/T_o < 2.0 \text{ then } \rho = 1.201 \exp(0.238\, T/T_o) \\ \text{if } 2.0 \le T/T_o < 3.0 \text{ then } \rho = 1.098 \exp(-0.193\, T/T_o) \end{array}\right\}$ and $C_p = 4.187 [0.219 + 0.342 \times 10^{-2} [1.8(T + 273.15)] - 0.293 \times 10^{-5} [1.8(T + 273.15)]^2]$

r Calculations*

A ow ty ed	Rock $\rho_s C_p$ (kJ/m³ · °C; T < T_{boil} 10°C)	Rock $\rho_s C_p$ (kJ/m³ · °C; T > T_{boil} + 10°C)	Figure in Appendix A Showing How $\rho_s C_p$ Was Changed	ρAir in Room Pseudo Thermal Conductivity Used (W/m · °C)	Waste Thermal Conductivity (W/m · °C)	Air ρC_p (kJ/m³ · °C)	Waste ρC_p (kJ/m³ · °C)	Initial In Situ Temperature at Repository Horizon (°C)	Backfill Parameter	Backfill Thermal Conductivity W/m · °C and T < T_{boil} 10°C	Backfill Thermal Conductivity W/m · °C and T > T_{boil} + 10°C	Figure in Appendix A Showing How Backfill Thermal Conductivity Was Changed	Backfill ρC_p kJ/m³ · °C for Saturated Conditions and T < T_{boil} 10°C	Backfill ρC_p kJ/m³ · °C for Dry Conditions and T > T_{boil} + 10°C	Figure in Appendix A Showing How Backfill ρC_p Was Changed	Investigator	Reference
	3.64E3	1.72E3	A-4	25	1.21	1.00	2.5E3	35	Saturated	1.18	0.48	A-3	4.77E3	8.37E2	A-4	SNL	15
	3.64E3	1.72E3	A-4	25	1.21	1.00	2.5E3	35	Saturated	1.18	0.48	A-3	4.77E3	8.37E2	A-4	SNL	15
	3.64E3	1.72E3	A-4	25	1.21	1.00	2.5E3	35	Dry	0.48	0.48	—	8.37E2	8.37E2	-	SNL	15
	3.64E3	1.72E3	A-4	25	1.21	1.00	2.5E3	35	Saturated	1.18	0.48	A-3	4.77E3	8.37E2	A-4	SNL	15
	3.64E3	1.72E3	A-4	25	1.21	1.00	2.5E3	35	Saturated	1.18	0.48	A-3	4.77E3	8.37E2	A-4	SNL	15
	3.64E3	1.72E3	A-4	25	1.21	1.00	2.5E3	35	Dry	0.48	0.48	--	8.37E2	8.37E2		SNL	15
	3.64E3	1.72E3	A-4	25	1.21	1.00	2.5E3	35	Saturated	1.18	0.48	A-3	4.77E3	8.37E2	A-4	SNL	15
	3.64E3	1.72E3	A-4	25	1.21	1.00	2.5E3	35	Saturated	1.18	0.48	A-3	4.77E3	8.37E2	A-4	SNL	15
	3.64E3	1.72E3	A-4	25	1.21	1.00	2.5E3	35	Saturated	1.18	0.48	A-3	4.77E3	8.37E2	A-4	SNL	15
	3.64E3	1.72E3	A-4	25	1.21	1.00	2.5E3	35	Dry	0.48	0.48		8.37E2	8.37E2		SNL	15
	3.64E3	1.72E3	A-4	25	1.21	1.00	2.5E3	55	Saturated	1.18	0.48	A-3	4.77E3	8.37E2	A-4	SNL	15
	3.64E3	1.72E3	A-4	25	1.21	1.00	2.5E3	55	Saturated	1.18	0.48	A-3	4.77E3	8.37E2	A-4	SNL	15
	3.64E3	1.72E3	A-4	25	1.21	1.00	2.5E3	55	Saturated	1.18	0.48	A-3	4.77E3	8.37E2	A-4	SNL	15
	3.64E3	1.72E3	A-4	25	1.21	1.00	2.5E3	55	Saturated	1.18	0.48	A-3	4.77E3	8.37E2	A-4	SNL	15
	3.64E3	1.72E3	A-2	55,61**	(A)	(C)	(B)	35	None	--	—					RE/SPEC	6

73.15)] 0.293 x 10^{6}[1.8(T + 273.15)]²

Table B–3. Summary of All Parameters Input in Very-Near-Field Calculations*

Type of Model	Waste Form	Thermal Loading (kW/acre)	Can Loading (kW/can)	Boiling Parameter (°C)	ER (%)	Time Range (yr)	Rock Thermal Conductivity (W/m · °C; T ≤ 90°C)	Rock Thermal Conductivity (W/m · °C; T > 110°C)	Figures in Appendix A Showing How Thermal Conductivity Was Changed	Rock $\rho_R C_p$ (kJ/m³ · °C; T ≤ 90°C)	Rock $\rho_R C_p$ (kJ/m³ · °C; T > 110°C)	Figures in Appendix A Showing How $\rho_R C_p$ Was Changed	Air Gap Pseudo-Thermal Conductivity for Radiation (W/m · °C)	Air in Room Pseudo Thermal Conductivity for Radiation (W/m · °C)	Air ρC_p (kJ/m³ · °C)	Waste Th Conduct (W/m
3-D	SF	75	0.55	No boil	10,20,30	0 - 100	2.4	2.4	--	3.64E3	3.64E3	--	0.13 - 1.3	55	(C)	(A)
3-D	SF	25,75,100,150	0.55	100	20	0 - 100	2.4	1.65	A-1	3.64E3	1.72E3	A-2	0.13 - 1.3	46,55,61,70**	(C)	(A)
3-D	SF	150	0.55	No boil	20	0 - 100	2.4	1.65	--	3.64E3	3.64E3	--	0.13 - 1.3	70	(C)	(A)
3-D	SF	50,75,100	0.55	100	20	0 - 100	2.4	1.55	A-1	3.64E3	1.72E3	A-2	0.13 - 1.3	50,55,61**	(C)	(A)
3-D	SF	50,75,100	0.55	No boil	20	0 - 100	2.4	2.4	--	3.64E3	3.64E3	--	0.13 - 1.3	50,55,61**	(C)	(A)
2-D axisymmetric	CHLW	75	1,2.16,3.5	100	20	0 - 100	1.92-2.88	1.32-1.98	A-7	3.64E3	1.72E3	A-8	25	25	1.76	1.21
2-D axisymmetric	CHLW	75	1,2.16,3.5	100	20	0 - 100	2.4	1.65	A-7	3.64E3	1.72E3	A-8	25	25	1.76	1.21
2-D axisymmetric	CHLW	75	1.0	100	20	0 - 100	1.1	0.74	A-7	3.72E3	1.38E3	A-8	25	25	1.76	1.21
2-D axisymmetric	CHLW	50,75,100	2.16	100	20	0 - 100	2.4	1.65	A-7	3.64E3	1.72E3	A-8	25	25	1.76	1.21
3-D	CHLW	75,100	2.16	100	20	0 - 100	2.4	1.55	A-7	3.64E3	1.715E3	A-8	0.10 - 0.46	22.1 - 37.1	1.0	1.20
3-D	CHLW	75,100	2.16	No boil	20	0 - 100	2.4	2.4	--	3.64E3	3.64E3	--	0.10 - 0.39	22.1 - 40.2	1.0	1.20

*The 3-D Calculations in Table B-3 include the room and pillar.
**Listed in the order used for various GTLs.

(A) $0.211 \cdot \left(\frac{T + 273}{100}\right)^{1.97}$ = K in W/m · °C, T = °C

(B) $4.194\,[689.2 + 13.38\,(T/100)]$ = ρC_p in kJ/m³ · °C, T = °C

(C) if $0 \le T/T_o < 1.0$ then $\rho = 1.289 \exp(-0.31\,T/T_o)$
if $1.0 < T/T_o < 2.0$ then $\rho = 1.201 \exp(-0.238\,T/T_o)$
if $2.0 \le T/T_o \le 3.0$ then $\rho = 1.098 \exp(-0.193\,T/T_o)$
and $C_p = 4.187\,[0.219 + 0.342 \times 10^{-4}(1.8(T + 273.15)) - 0.293 \times 10^{-7}(1.8(T + 273.15))^2]$

J Calculations*

	Rock Thermal Conductivity (W/m · °C; T <90°C)	Rock Thermal Conductivity (W/m · °C; T >110°C)	Figures in Appendix A Showing How Thermal Conductivity Was Changed	Rock $\rho_R C_p$ (kJ/m³ · °C; T <90°C)	Rock $\rho_R C_p$ (kJ/m³ · °C; T >110°C)	Figures in Appendix A Showing How $\rho_R C_p$ Was Changed	Air Gap Pseudo-Thermal Conductivity for Radiation (W/m · °C)	Air in Room Pseudo Thermal Conductivity for Radiation (W/m · °C)	Air ρC_p (kJ/m³ · °C)	Waste Thermal Conductivity (W/m · °C)	Waste ρC_p (kJ/m³ · °C)	Initial In Situ Temperature (°C)	Investigator	Reference
0	2.4	2.4	—	3.64E3	3.64E3	—	0.13 - 1.3	55	(C)	(A)	(B)	55	RE/SPEC	6
0	2.4	1.65	A-1	3.64E3	1.72E3	A-2	0.13 - 1.3	46,55,61,70**	(C)	(A)	(B)	55	RE/SPEC	6
0	2.4	1.65	—	3.64E3	3.64E3	—	0.13 - 1.3	70	(C)	(A)	(B)	55	RE/SPEC	6
0	2.4	1.55	A-1	3.64E3	1.72E3	A-2	0.13 - 1.3	50,55,61**	(C)	(A)	(B)	35	RE/SPEC	6
0	2.4	2.4	—	3.64E3	3.64E3	—	0.13 - 1.3	50,55,61**	(C)	(A)	(B)	35	RE/SPEC	6
0	1.92-2.88	1.32-1.98	A-7	3.64E3	1.72E3	A-8	25	25	1.76	1.21	2.50E3	55	SNL	15
0	2.4	1.65	A-7	3.64E3	1.72E3	A-8	25	25	1.76	1.21	2.50E3	55	SNL	15
0	1.1	0.74	A-7	3.72E3	1.38E3	A-8	25	25	1.76	1.21	2.50E3	55	SNL	15
0	2.4	1.65	A-7	3.64E3	1.72E3	A-8	25	25	1.76	1.21	2.50E3	35	SNL	15
0	2.4	1.55	A-7	3.64E3	1.715E3	A-8	0.10 - 0.46	22.1 - 37.1	1.0	1.20	2.50E3	35	SNL	16
0	2.4	2.4	—	3.64E3	3.64E3	—	0.10 - 0.39	22.1 - 40.2	1.0	1.20	2.50E3	35	SNL	16

^{2} x 10^{-4}[1.8(T + 273.15)] 0.293 x 10^{-4}[1.8(T + 273.15)]^{2}]

DISTRIBUTION:

TIC-4500-R69 UC-70 (325)

US Department of Energy
Office of Waste Isolation
Room B-207
Germantown, MD 20767
Attn: C. A. Heath, Director

US Department of Energy
Technology Team
Room B-220
Germantown, MD 20767
Attn: D. L. Vieth, Acting Team Leader

US Department of Energy
National Waste Terminal
Storage Program Office
505 King Avenue
Columbus, OH 43201
Attn: J. O. Neff, Program Manager

Lawrence Livermore National Lab
University of California
PO Box 808
Mail Stop L-204
Livermore, CA 94550
Attn: L. D. Ramspott
Technical Project Officer

Los Alamos National Laboratory
University of California
PO Box 1663
Mail Stop 514
Los Alamos, NM 87545
Attn: B. R. Erdal
Technical Project Officer

Westinghouse - AESD
PO Box 708
Mail Stop 703
Mercury, NV 89023
Attn: A. R. Hakl, Site Manager

US Geological Survey (2)
Post Office Box 25046
Mail Stop 954
Federal Center
Denver, CO 80301
Attn: G. L. Dixon, Technical Project Officer
W. E. Wilson

W. S. Twenhofel
820 Estes Street
Lakewood, CO 80226

US Department of Energy
Office of Waste Isolation
Room B-214
Germantown, MD 20767
Attn: C. R. Cooley, Deputy Director

US Department of Energy
Richland Operations Office
PO Box 550
Richland, WA 99352
Attn: R. G. Goranson

Rockwell International Atomics
International Division
Rockwell Hanford Operations
Richland, WA 99352
Attn: R. Deju

US Department of Energy (13)
PO Box 14100
Las Vegas, NV 89114
Attn: R. M. Nelson, Jr., Director of
Waste Management Project Office (3)
D. F. Miller, Director of Office of
Public Affairs
R. H. Marks, CP-1, MS 210
B. W. Church, Director of
Health Physics Div
R. R. Loux, (7)

Holmes & Narver, Inc.
PO Box 14340
Las Vegas, NV 89114
Attn: A. E. Gurrola

Lawrence Livermore National Laboratory
University of California
Mail Stop L-209
PO Box 808
Livermore, CA 94550
Attn: K. Street, Jr.

Los Alamos National Laboratory
Mail Stop 760
PO Box 1663
Los Alamos, NM 87545
Attn: D. C. Hoffman

DISTRIBUTION (cont):

Battelle (7)
Office of Nuclear Waste Isolation
505 King Avenue
Columbus, OH 43201
Attn: N. E. Carter
S. Goldsmith
ONWI Library (5)

Battelle
Office of NWTS Integration
505 King Avenue
Columbus, OH 43201
Attn: W. A. Carbiener

State of Nevada (2)
Capitol Complex
Carson City, NV 89023
Attn: R. M. Hill, State Planning
Coordinator, Governer's
Office of Planning Coordination
N. A. Clark, Department of Energy

International Atomic Energy Agency
Div of Nuclear Power & Reactors
Karnter Ring 11
PO Box 590, A-1011
Vienna, AUSTRIA
Attn: J. P. Colton

Reynolds Electrical & Engineering Co., Inc.
Mail Stop 555
PO Box 14400
Las Vegas, NV 89114
Attn: H. D. Cunningham

Fenix & Scisson, Inc.
PO Box 15408
Las Vegas, NV 89114
Attn: J. A. Cross

Argonne National Laboratories
9700 S. Cass Avenue
Argonne, IL 60439
Attn: A. M. Friedman

Texas A&M University
College of Engineering
College Station, TX 77840
Attn: J. Russell

RE/SPEC, Inc.
PO Box 725
Rapid City, SD 57709
Attn: P. Gnirk

US Nuclear Regulatory Commission
Washington, DC 20555
Attn: J. Greeves MS 697-SS

Westinghouse AESD (2)
PO Box 10864
Pittsburg, PA 15236
Attn: W. Lundburg
D. Newly

1417 F. W. Muller
4530 R. W. Lynch
4531 L. W. Scully
4537 J. R. Tillerson
4537 B. S. Langkopf (16)
4537 A. R. Lappin
4537 R. M. Zimmerman
4537 R. R. Peters
4537 D. R. Fortney
4537 R. Shaw
4538 R. C. Lincoln
4538 A. E. Stephenson
5511 J. W. Nunziato
Attn: R. R. Eaton
D. K. Gartling
5521 R. D. Krieg
Attn: R. K. Thomas
N. E. Gilbertsen
5522 R. L. Johnson
5532 B. M. Butcher
Attn: W. A. Olsson
5633 W. D. Sundberg
8214 M. A. Pound
3141 L. J. Erickson (5)
3151 W. L. Garner (3)

Reprinted August 1982

9762 B. S. Langkopf (100)

Org.	Bldg.	Name	Rec'd by	Org.	Bldg.	Name	Rec'd by

Sandia National Laboratories